NASA/CR-2005-213742

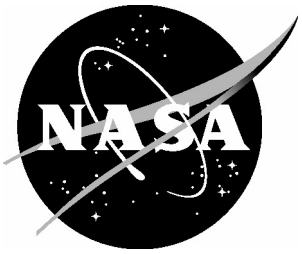

High Speed Research Program Sonic Fatigue Summary Report

Theodor H. Beier and Paul Heaton
The Boeing Company, St. Louis, Missouri

April 2005

The NASA STI Program Office . . . in Profile

Since its founding, NASA has been dedicated to the advancement of aeronautics and space science. The NASA Scientific and Technical Information (STI) Program Office plays a key part in helping NASA maintain this important role.

The NASA STI Program Office is operated by Langley Research Center, the lead center for NASA's scientific and technical information. The NASA STI Program Office provides access to the NASA STI Database, the largest collection of aeronautical and space science STI in the world. The Program Office is also NASA's institutional mechanism for disseminating the results of its research and development activities. These results are published by NASA in the NASA STI Report Series, which includes the following report types:

- TECHNICAL PUBLICATION. Reports of completed research or a major significant phase of research that present the results of NASA programs and include extensive data or theoretical analysis. Includes compilations of significant scientific and technical data and information deemed to be of continuing reference value. NASA counterpart of peer-reviewed formal professional papers, but having less stringent limitations on manuscript length and extent of graphic presentations.

- TECHNICAL MEMORANDUM. Scientific and technical findings that are preliminary or of specialized interest, e.g., quick release reports, working papers, and bibliographies that contain minimal annotation. Does not contain extensive analysis.

- CONTRACTOR REPORT. Scientific and technical findings by NASA-sponsored contractors and grantees.

- CONFERENCE PUBLICATION. Collected papers from scientific and technical conferences, symposia, seminars, or other meetings sponsored or co-sponsored by NASA.

- SPECIAL PUBLICATION. Scientific, technical, or historical information from NASA programs, projects, and missions, often concerned with subjects having substantial public interest.

- TECHNICAL TRANSLATION. English-language translations of foreign scientific and technical material pertinent to NASA's mission.

Specialized services that complement the STI Program Office's diverse offerings include creating custom thesauri, building customized databases, organizing and publishing research results ... even providing videos.

For more information about the NASA STI Program Office, see the following:

- Access the NASA STI Program Home Page at ***http://www.sti.nasa.gov***

- E-mail your question via the Internet to help@sti.nasa.gov

- Fax your question to the NASA STI Help Desk at (301) 621-0134

- Phone the NASA STI Help Desk at (301) 621-0390

- Write to:
  NASA STI Help Desk
  NASA Center for AeroSpace Information
  7121 Standard Drive
  Hanover, MD 21076-1320

NASA/CR-2005-213742

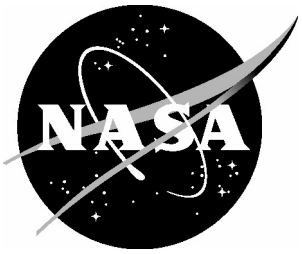

High Speed Research Program Sonic Fatigue Summary Report

Theodor H. Beier and Paul Heaton
The Boeing Company, St. Louis, Missouri

National Aeronautics and
Space Administration

Langley Research Center
Hampton, Virginia 23681-2199

Prepared for Langley Research Center
under Contract NAS1-20220

April 2005

Available from:

NASA Center for AeroSpace Information (CASI)
7121 Standard Drive
Hanover, MD 21076-1320
(301) 621-0390

National Technical Information Service (NTIS)
5285 Port Royal Road
Springfield, VA 22161-2171
(703) 605-6000

Table of Contents

List of Figures

List of Tables

1.0 EXECUTIVE SUMMARY

Introduction

The objective of this sonic fatigue summary is to provide major findings and technical results of studies, initiated in 1994, to assess sonic fatigue behavior of structure that is being considered for the High Speed Civil Transport (HSCT). High Speed Research (HSR) program objectives in the area of sonic fatigue were to:

1. predict inlet, exhaust and boundary layer acoustic loads,
2. measure high cycle fatigue data for materials developed during the HSR program,
3. develop advanced sonic fatigue calculation methods to reduce required conservatism in airframe designs,
4. develop damping techniques for sonic fatigue reduction where weight effective,
5. develop wing and fuselage sonic fatigue design requirements, and
6. perform sonic fatigue analyses on HSCT structural concepts to provide guidance to design teams.

All goals were partially achieved, but none were completed due to the premature conclusion of the HSR program.

Summary of Major Program Findings

The following items are of interest to other segments of the HSR program.

1. IM7/PETI-5 Material Characterization: This material is extremely resistant to high cycle fatigue damage with allowable strains exceeding those for titanium. Figure 1 shows test results for coupon and representative joint test specimens. This material has little or no reduction in properties at 350^{o}F. It should be tested at temperatures up to 500^{o}F to determine its true limits.
2. Skin-Stringer Fuselage Concept: This concept, as designed, is very close to meeting requirements developed for sonic fatigue resistant structure. Sonic fatigue analyses were conducted on representative HSCT side fuselage sub-components to define structure with acceptable sonic fatigue life (60,000 hours times a scatter factor of 2) when subjected to the sonic design load, including a 3.5 dB factor of safety. Initial design curves, developed by NASTRAN linear

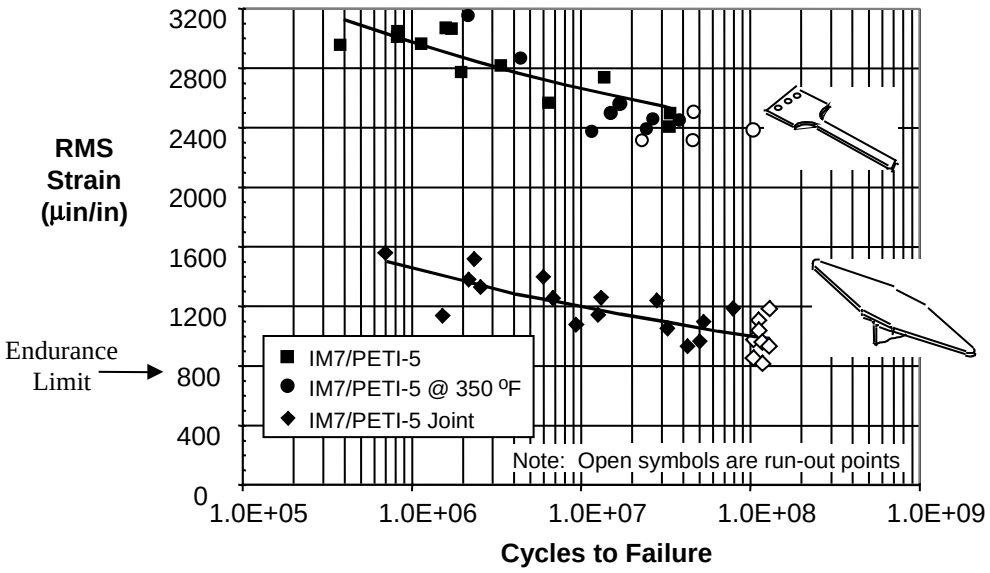

Figure 1 IM7/PETI-5 Fatigue Test Data

response parametric analyses, provide required thickness values for skin panels, stringer webs and stringer flange areas. These criteria were applied to the fuselage pathfinder designs. It was assumed that high acoustic impingement exists on the side of fuselage Section 43 due to a wake from the canard and on the sides and bottom of fuselage Section 46 as a result of engine exhaust noise. Minor changes were recommended in the areas below the window belt and passenger floor as shown in Table 1. This design concept could be improved significantly if the terminations in the stringer flanges were tapered. This would increase the endurance limit significantly and possibly remove most of the required structural gage increases recommended for sonic fatigue considerations.

Table 1 Recommended Changes in Skin-Stringer Design

Section	Detail	Current Design Thickness (in)	Required Thickness(in)	Δweight (lb/sq ft)
43	Tear Strap	0.04	0.05	0.014
46	Stringer Web	0.05	0.115	0.085

3. PMC-TI Honeycomb Concept: High cycle fatigue resistance of PMC-TI honeycomb structure is governed by its limited shear capability in the bond between the honeycomb and face sheet. This failure mechanism was identified by testing of honeycomb strip beams and verified by NASTRAN linear response vibration analyses of the strip beams and sonic fatigue analyses of panels. Design curves were developed from these analytic results and applied to representative HSCT panels. To accommodate this limited shear capability of the bond, core thickness

less than 0.5 inch and panel dimensions greater than 50 inches are to be avoided.

4. TU-144 Flight Data: Engine inlet and exhaust noise levels based on TU-144 flight data are much more severe than predictions based on tactical aircraft with supersonic capability, such as the F-15 and AV-8B (Figure 2). Sonic fatigue design requirements were, however, based on the lower tactical aircraft predictions because it is expected that an aircraft with the noise characteristics of the TU-144 would not be economically viable.

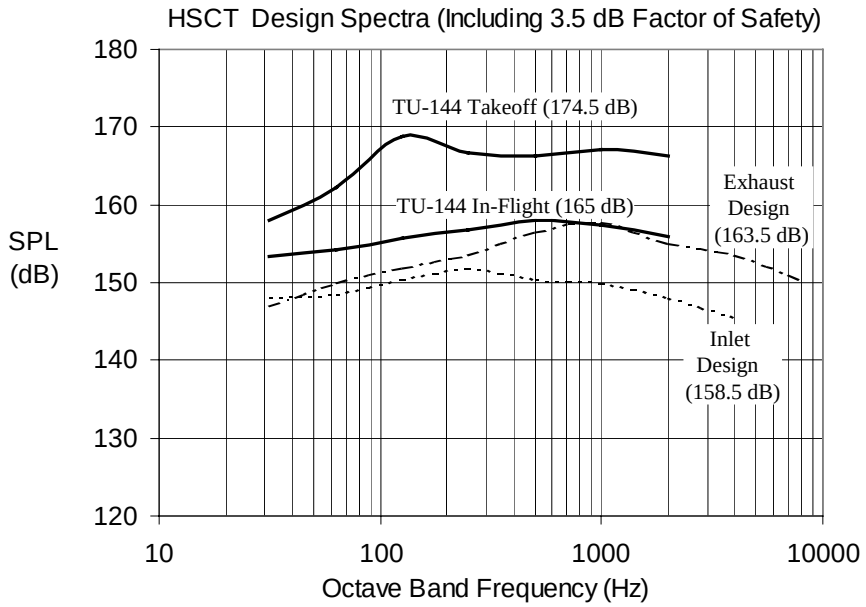

Figure 2 Comparison of Noise Spectra Based on TU-144 Data with HSR Design Spectra - Exhaust and Inlet

5. Addition of Damping to Structure: Because of the very high durability of IM7/PETI-5, the addition of viscous damping layers to reduce sonic fatigue is not weight effective for a skin-stringer fuselage. Increasing material gages or adding substructure, where required, seems to be more efficient. Damping techniques may be required, however, for other aircraft components, such as empennage or control surfaces, which were not analyzed in the present program.

Recommendations for Continued Effort

The HSR Sonic Fatigue program provided considerable useful information, which if extended, would be even more valuable. Despite cessation of this program, the following tasks are recommended for continuing effort.

1. Further reduction of the TU-144 flight data is required to determine the distribution of sonic loads on all high acoustic zones of the airframe, i.e., to develop a sonic load map of the airframe. Primary zones of interest include engine nacelles, trailing edge control surface and empennage. These data can then be scaled based on HSCT expected engine flow rates, areas and temperatures to yield more accurate sonic load predictions.

2. Further characterization of strain - cycles to failure (ε-n) data for IM7/PETI-5 material requires additional testing at elevated temperatures and with static pre-loads applied. Testing should be conducted at 500^{o}F because the reduction in properties at 350^{o}F (Figure 1) is within the scatter band of the room temperature data. These tests would enhance the possibility of this material being used on other programs.

3. Development of the NASTRAN DMAP solution for non-linear dynamic response and the life calculation nCode fatigue module should be completed as a basis for the performance of more accurate sonic fatigue analyses. Current linear analysis and the resulting uncertainties in results lead to conservative, relatively heavy designs. These improved methods are needed for programs other than HSR and would be of immediate value.

4. Sonic fatigue analyses should continue in support of the structural design efforts which continue, in order to evaluate critical fatigue details in the design concepts. These include the close-outs at the edges of PMC-TI honeycomb panels which are prone to adhesive shear failures in areas of high dynamic response of large panels.

2.0 SONIC LOADING

The primary sources of sonic loading applicable to side fuselage and wing panels are inlet duct propagated noise, propulsion exhaust noise and turbulent wakes from body protuberances. The objective of this task was to predict appropriate sonic loading based on available data and to validate that loading with TU-144 flight test data.

Inlet Noise Prediction

Predicted overall sound pressure level noise contours on the fuselage and wing surfaces due to engine inlet noise propagation were determined and are shown in Figure 3. The spectrum shape shown in Figure 4 and overall noise levels inside the inlet were based on measured data from supersonic tactical aircraft. More details of this effort may be found in References [a] and [b]. These acoustic levels were used for preliminary sonic fatigue calculations on the lower surface of the wing and strake to determine required structural sizing. Flight test data from the TU-144 flight program were analyzed and compared to these predictions.

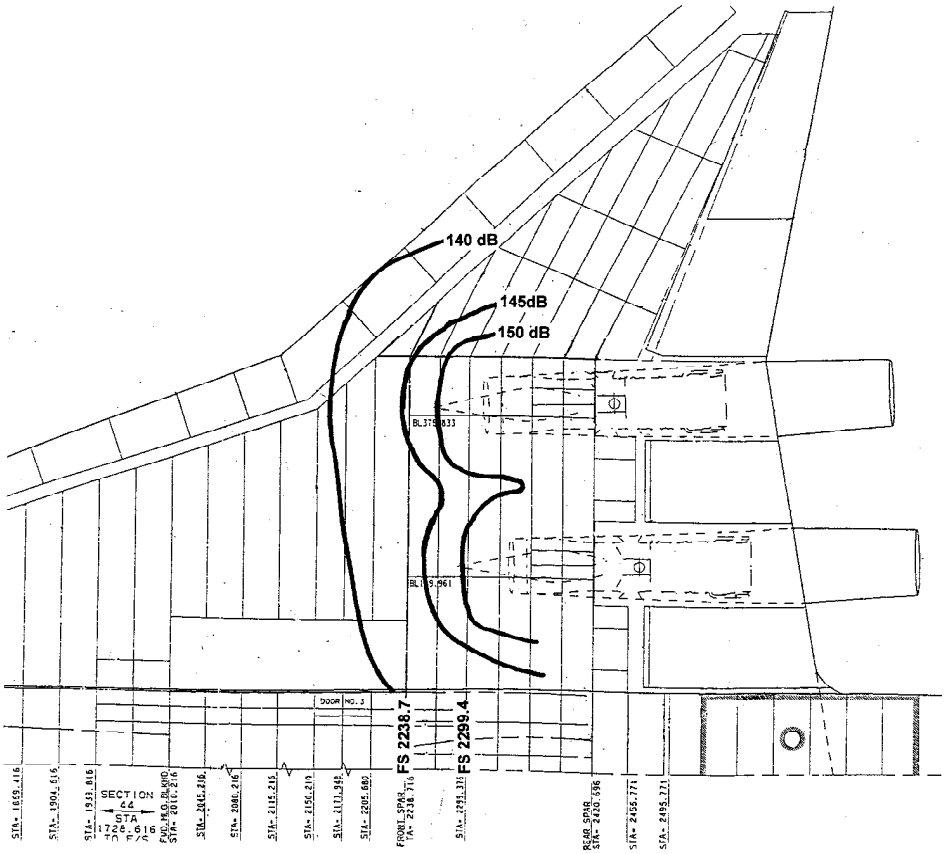

Figure 3 Engine Inlet Duct Propagated Noise Levels

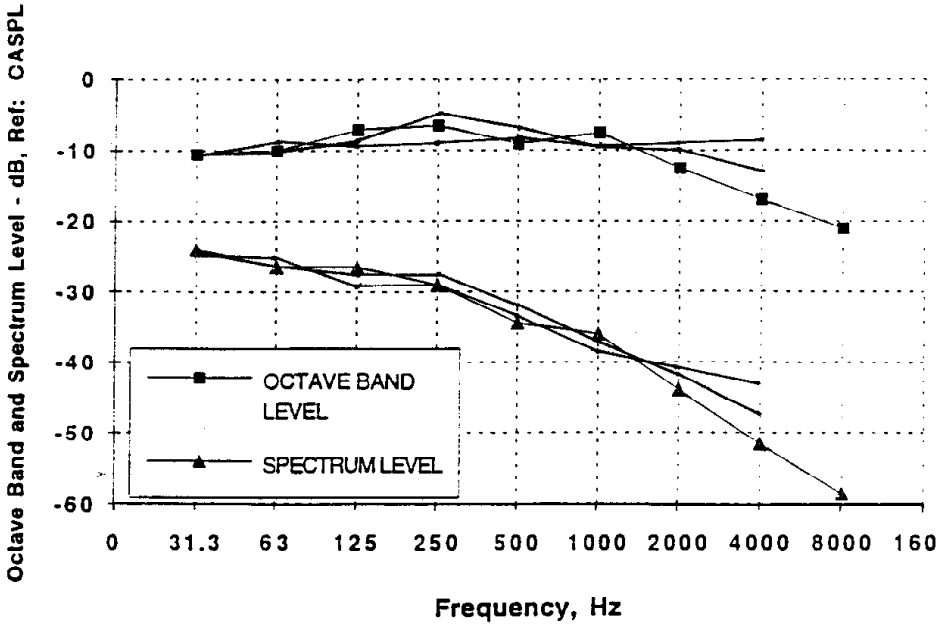

Figure 4 Engine Inlet Spectrum

Exhaust Noise Prediction

The maximum predicted exhaust noise, shown in Figure 5 with the previously discussed inlet noise contours, is assumed to be 160 dB OASPL with spectral content based on AV-8B Harrier aircraft measurements [Reference c]. AV-8B data were selected as the most appropriate of those currently available. As shown in Figure 6, the predicted exhaust levels are higher than inlet noise levels for all frequencies and are, therefore, used in development of HSR sonic fatigue design requirements for fuselage structure.

When utilized for sonic fatigue design and analysis, these predicted levels are increased by 3.5 dB to comply with a factor of safety requirement of 1.5 on sonic pressure. The resulting 163.5 dB exhaust noise OASPL is to be applied for twice the HSCT service life requirement of 60,000 hours. For preliminary sizing analyses, panel thickness needed to assure an infinite life at the material strain limit was determined, exceeding this service life criterion. Figure 7 shows the assumed exhaust noise octave band sound pressure level (SPL) and the corresponding spectrum level (SL) sonic loading. The narrow band SL, defined for 1 Hz bandwidth, is used for sonic fatigue life calculations since the assumed failure mechanism is high cycle fatigue at structural resonant frequencies. These noise levels, based on AV-8B exhaust measurements [Reference c], should be updated based on TU-144 data [Reference d] analyses.

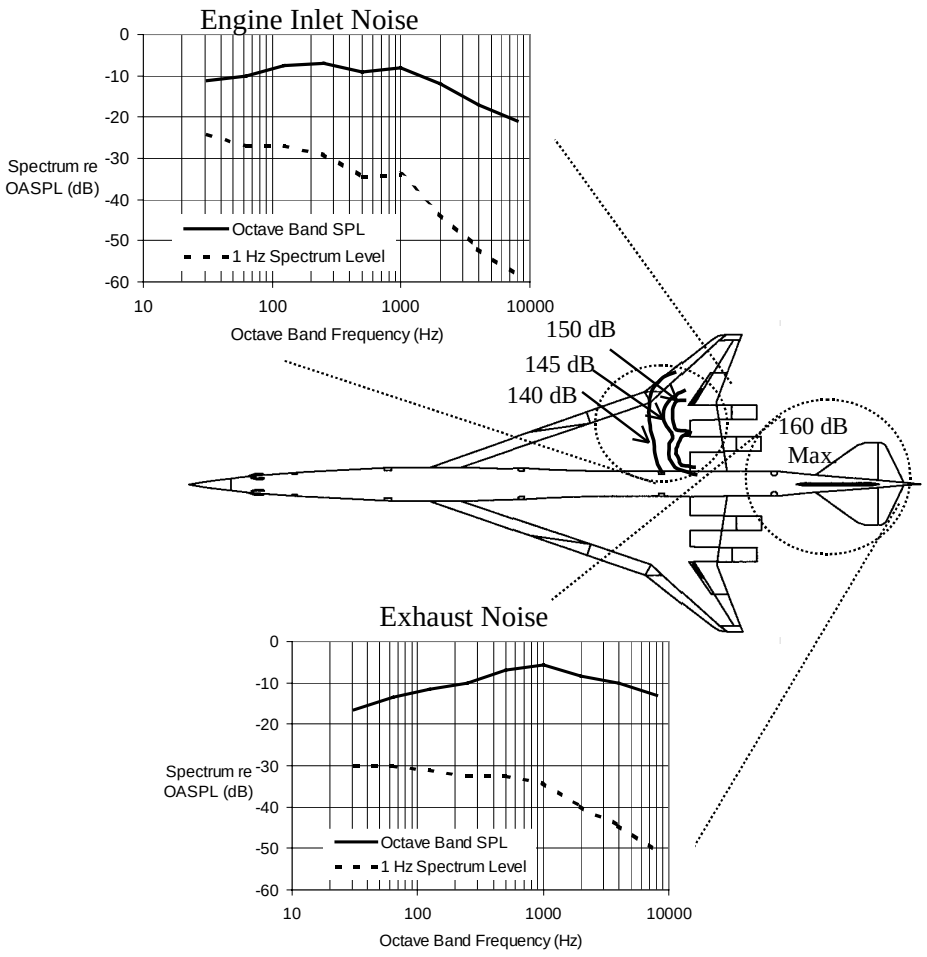

Figure 5 HSCT Engine Inlet and Exhaust Noise

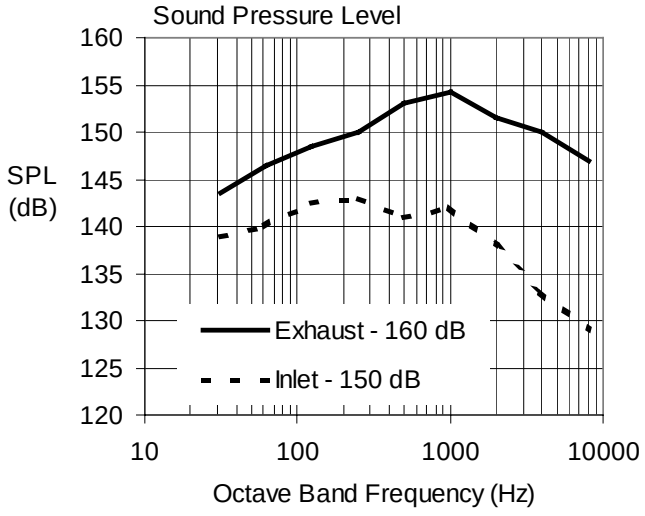

Figure 6 Comparison of HSCT Engine Inlet and Exhaust Noise Levels

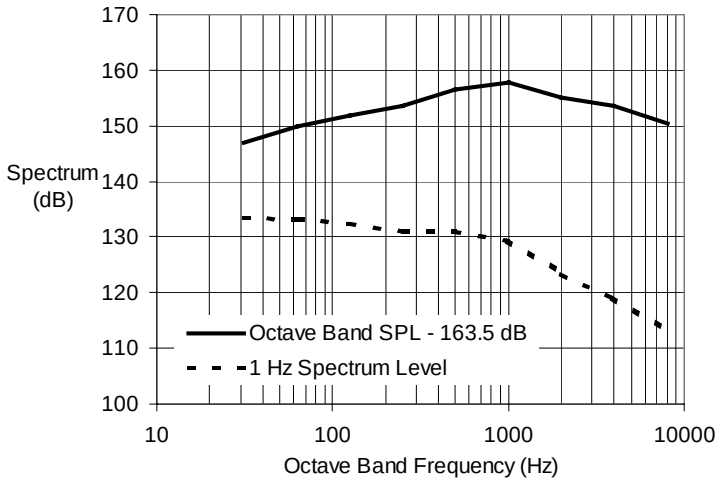

Figure 7 Sonic Loading for Fuselage Design

TU-144 Data Analysis

TU-144 flight tests were conducted in Russia during 1997 and 1998 with conditions shown in Figure 8. Twelve acoustic gages were employed to measure sonic pressures on airframe structure impinged upon by inlet and exhaust noise loading. Two gages were mounted on the tail, two on the lower rudder, two on the elevon and six on surfaces adjacent to the inlet duct. Gage locations are shown in Figure 9.

Flight No.	Date	Conditions
9	8/10/97	subsonic, low altitude
10	10/29/97	supersonic (M 1.2-1.98), above 11,400 m.
11	11/14/97	supersonic (up to M 1.78), above 10,000 m
16	1/22/98	high subsonic (M 0.9), 9000 m.
17	1/29/98	supersonic (M 1.0 - 1.985)

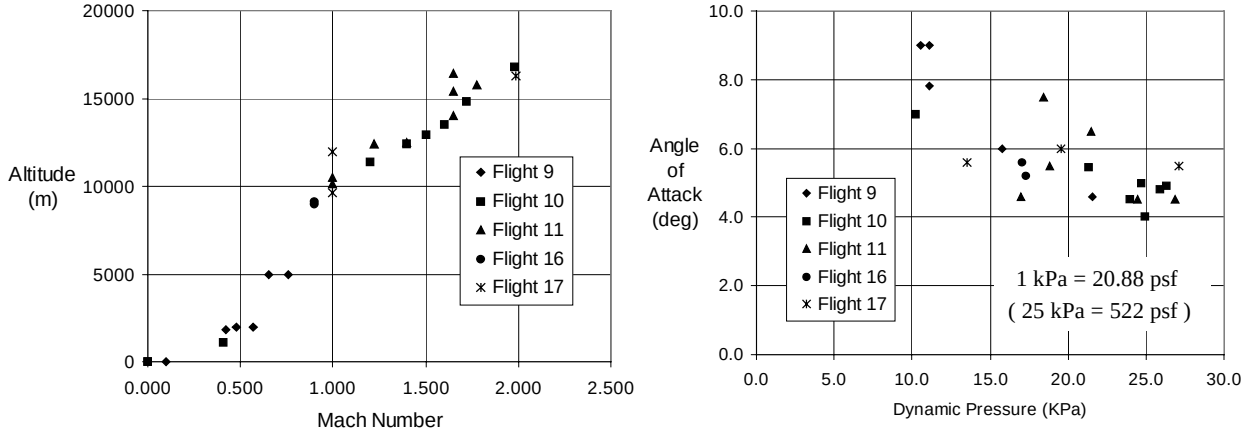

Figure 8 TU-144 Flight Test Conditions

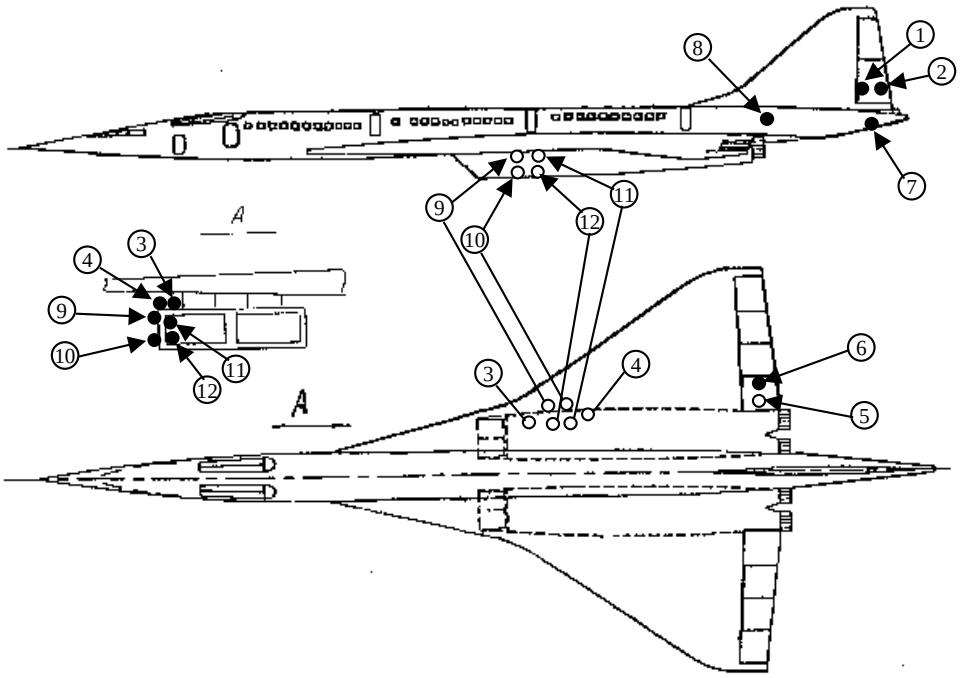

Category	Gage	Location
Exhaust Noise	7	Fuselage tailcone
	8	Fuselage tail section
	1	Lower rudder
	2	Lower rudder
	5	Lower right inner elevon
	6	Upper right inner elevon
Inlet Noise	3	Outer Surface - Top
	4	Outer Surface - Top
	9	Outer Surface - Upper Side
	10	Outer Surface - Lower Side
	11	Inner Surface - Upper Side
	12	Inner Surface - Lower Side

Figure 9 TU-144 Acoustic Gages

The procedure used in preliminary data analysis of TU-144 external noise measurements was:

1. Measured pressure power spectral density (PSD) plots were converted to one third octave band sound pressure level (SPL) curves for all gages and flight conditions. Overall sound pressure level (OASPL) was computed for each SPL.

2. The SPL spectra were combined and enveloped based on the location (either exhaust or inlet as categorized in Figure 9) and on the flight condition. Flight conditions were segregated into four categories: takeoff/landing, subsonic flight, low supersonic flight (dynamic pressure q less than 20 kPa), and high supersonic flight (q > 20 kPa). This process resulted in eight SPL spectra (2 locations x 4 flight categories).
3. The SPL envelopes were adjusted so that each computed OASPL matched the maximum measured OASPL for the appropriate location and flight condition.
4. A 3.5 dB factor of safety was applied for design purposes.

The resulting exhaust and inlet noise spectra, based on TU-144 flight data, are shown in Figures 10 and 11. Highest noise levels (> 170 dB OASPL) were measured at exhaust impingement gages on the tailcone and rudder during takeoff. Less spread among flight conditions was noted for inlet design spectra (161.6 to 164.9 dB) than for exhaust data (156.8 to 174.5 dB). The greatest variation in exhaust data is due to the magnitude of the take-off level, which can be greatly affected by the use of afterburners and by take-off weight.

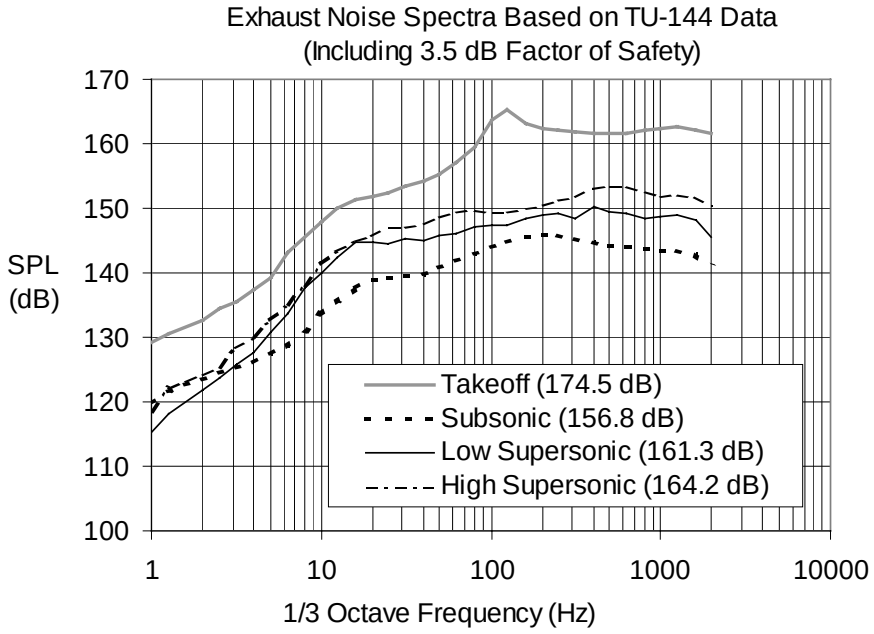

Figure 10 Exhaust Noise Design Spectra Based on TU-144 Data

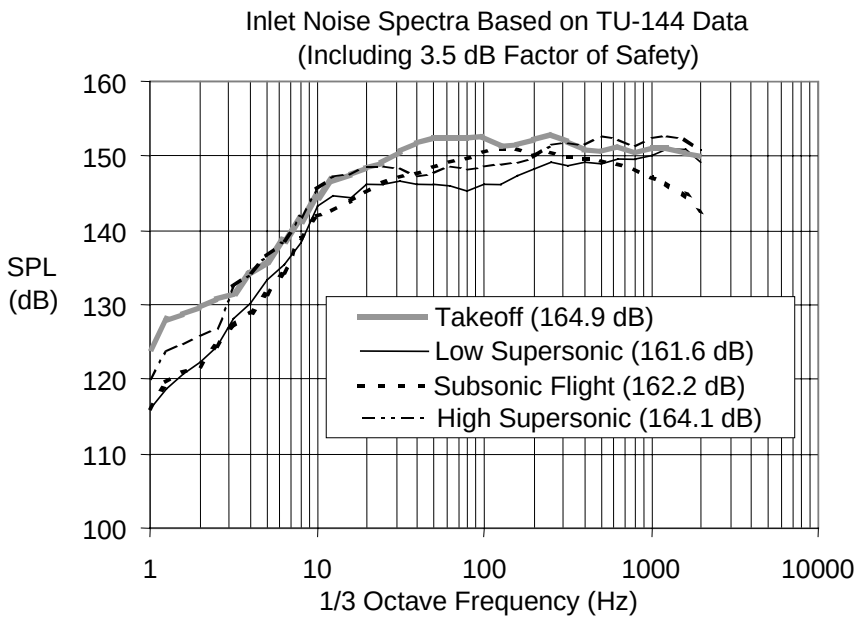

Figure 11 Inlet Noise Design Spectra Based on TU-144 Data

Comparisons of exhaust and inlet noise spectra are shown in Figures 12, 13 and 14. Exhaust levels were much higher than those at the inlet during takeoff conditions. Inlet levels exceed exhaust noise by up to 6 dB during subsonic flight. Levels during supersonic flight appear relatively independent of specific mach/altitude conditions and gage locations.

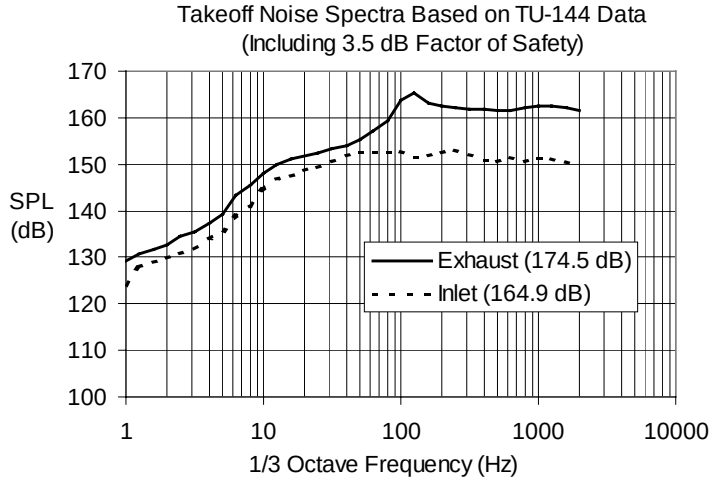

Figure 12 TU-144 Exhaust vs. Inlet Noise - Takeoff

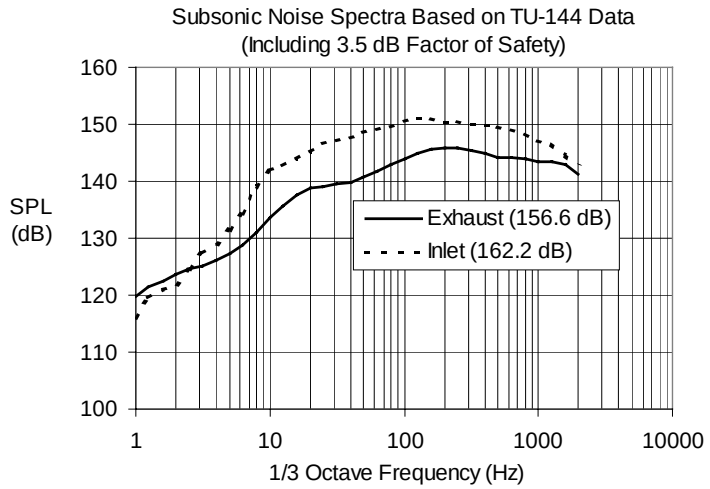

Figure 13 TU-144 Exhaust vs. Inlet Noise - Subsonic Flight

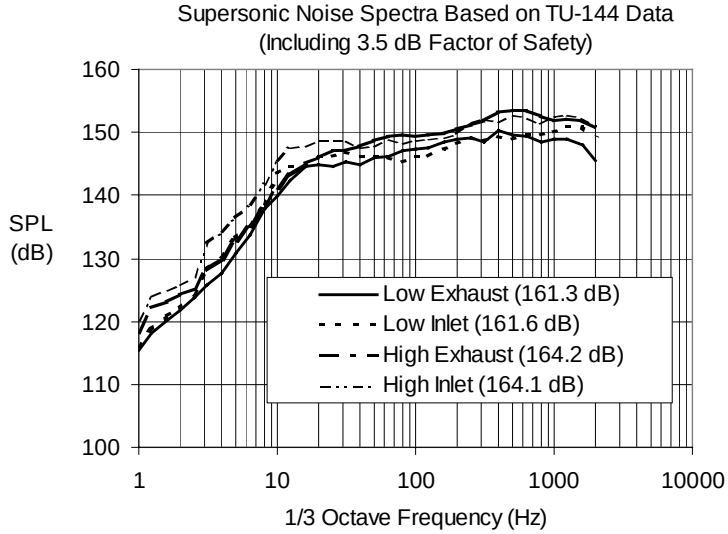

Figure 14 TU-144 Exhaust vs. Inlet Noise - Supersonic Flight

Preliminary analysis of the TU-144 flight data indicates that sonic loading higher than that predicted, and utilized in HSCT fuselage and wing sonic fatigue analyses, may be expected during actual flight. As shown in Figure 15,TU-144 in-flight levels are slightly higher than the assumed design levels (2-4 dB) while takeoff levels are as much as 10 dB higher. However, despite TU-144 results, preliminary sonic fatigue design requirements were still based on the lower tactical aircraft predictions because it is expected that an aircraft with the noise characteristics of the TU-144 would not be economically viable. Furthermore, the turbojet engines used on the TU-144 research aircraft were not the original equipment. The aircraft was retrofitted with more powerful engines from the Blackjack bomber.

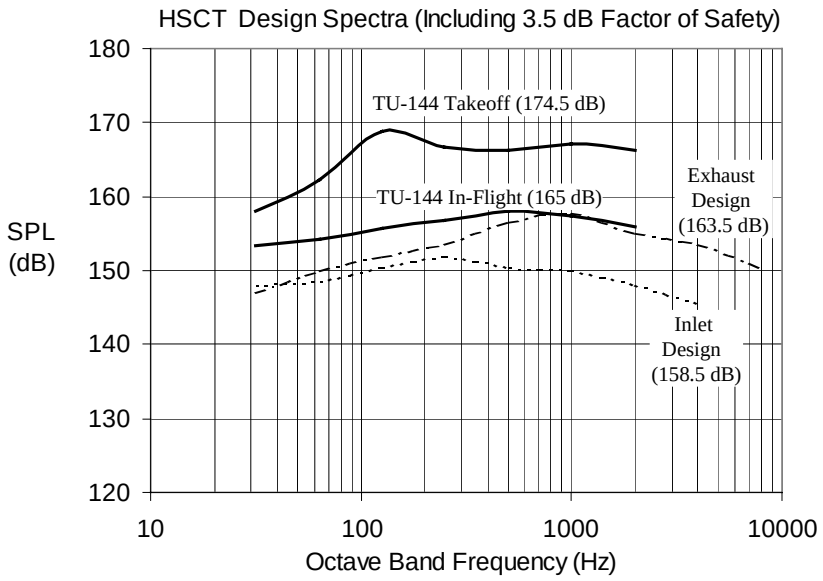

Figure 15 TU-144 Data vs. Preliminary HSCT Design Spectra

Additional Recommended Data Reduction

Further reduction of the TU-144 flight data is required to determine the distribution of sonic loads on all high acoustic zones of the airframe, i.e., to develop a sonic load map of the airframe. These data can then be scaled based on HSCT expected engine flow rates, areas and temperatures to yield more accurate sonic load predictions. Preliminary analyses of two zones of interest - trailing edge control surface and empennage areas - have been performed for the TU-144 data. Data measured by gages 5 and 6 on the right inner elevon were used to develop trailing edge control surface sound pressure levels. Gage 1 and 2 data were similarly used for empennage sound levels. Table 2 summarizes the maximum overall sound pressure levels measured for these zones as well as those previously presented for areas with exhaust and inlet noise impingement. A 3.5 dB factor of safety is applied

Table 2 Summary of OASPL Values from TU-144 Data

	Overall Sound Pressure Level (dB)			
	Takeoff	Subsonic Flight	Low Supersonic	High Supersonic
TE Control Surface	145.3	145.3	154.1	149.4
Empennage	164.5	149.2	152.8	149.4
Exhaust Areas	171.0	153.3	157.8	160.7
Inlet Noise	161.4	158.7	158.1	160.6

to these values to define design spectra. Figures 16 and 17 present the sound pressure level spectra developed for the trailing edge control surface and empennage areas for the four flight condition categories. Further evaluation of these and other areas of high sonic loading is recommended.

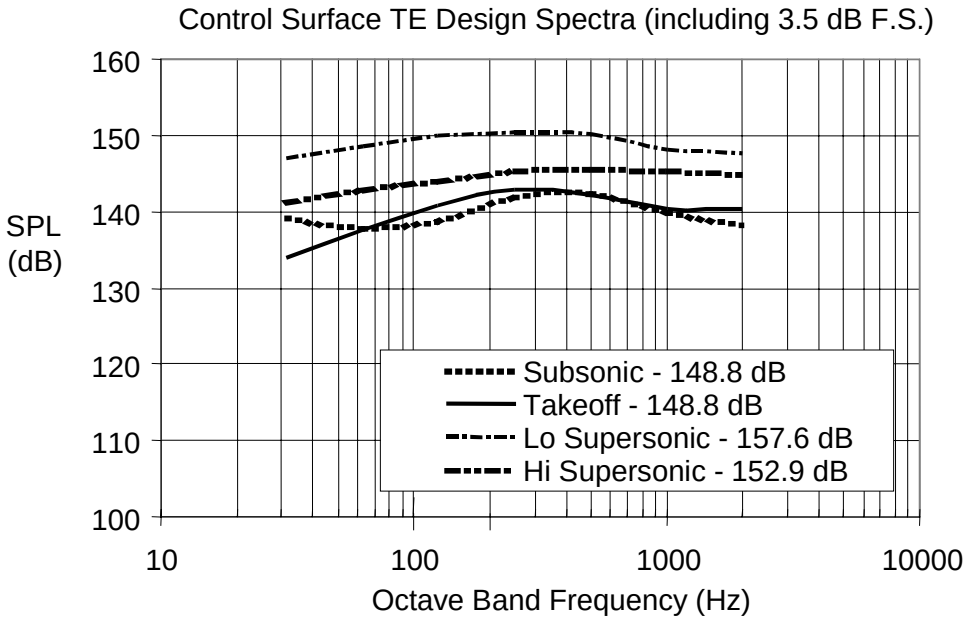

Figure 16 Trailing Edge Control Surface SPL Based on TU-144 Data

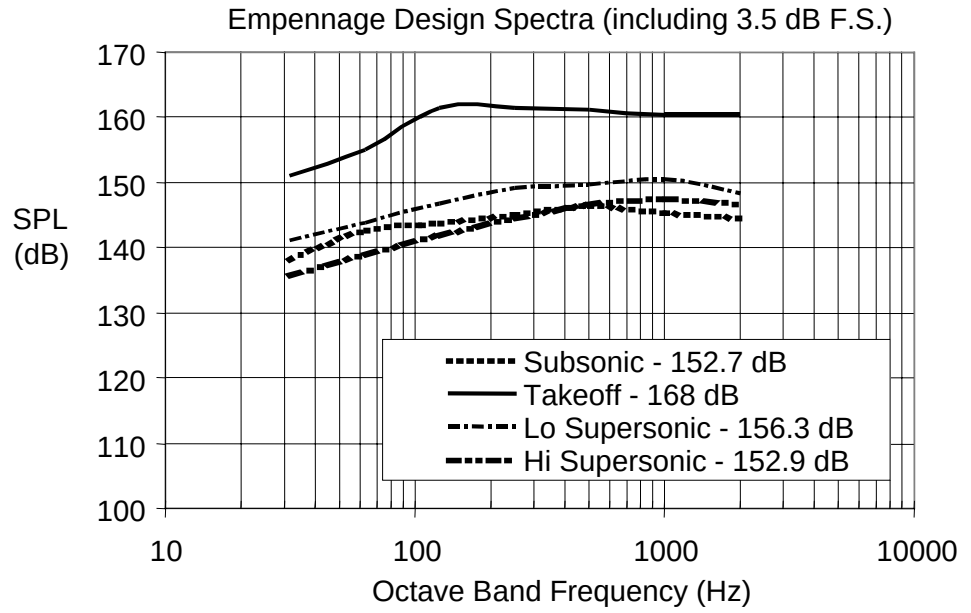

Figure 17 Empennage SPL Based on TU-144 Data

3.0 MATERIALS CHARACTERIZATION

Material characterization for HSR sonic fatigue efforts included both sub-component testing and high cycle fatigue testing of coupons and joint specimens. The objective of this task was to conduct tests needed to define material allowable strains for sonic fatigue analyses.

Sub-component Testing

In order to evaluate the sonic fatigue characteristics of candidate structures, two candidate panel concepts were chosen to be tested in NASA-LARC Thermal Acoustic Facility Apparatus (TAFA) in 1997. Since less is known about acoustic fatigue of honeycomb panels, both candidates tested were honeycomb core panels with face sheets.

ASTECH Titanium Core Panel

The first panel was a 26.0 x 26.0 inch ASTECH titanium 1.0 inch core panel with 0.014 inch thick titanium facesheets. This structure is produced by metallurgically bonding the face sheets to the titanium core. A sketch showing the cross section of the panel is shown in Figure 18. A finite element model was prepared to predict the modal frequencies of the panel to assure that it was within the testable range of the facility. The analytical model was run with two different edge conditions to provide bounds on the frequency. A modal test was performed on the panel while installed in the wall of the chamber. Table 3 shows the summary of predicted versus measured frequencies for each mode.

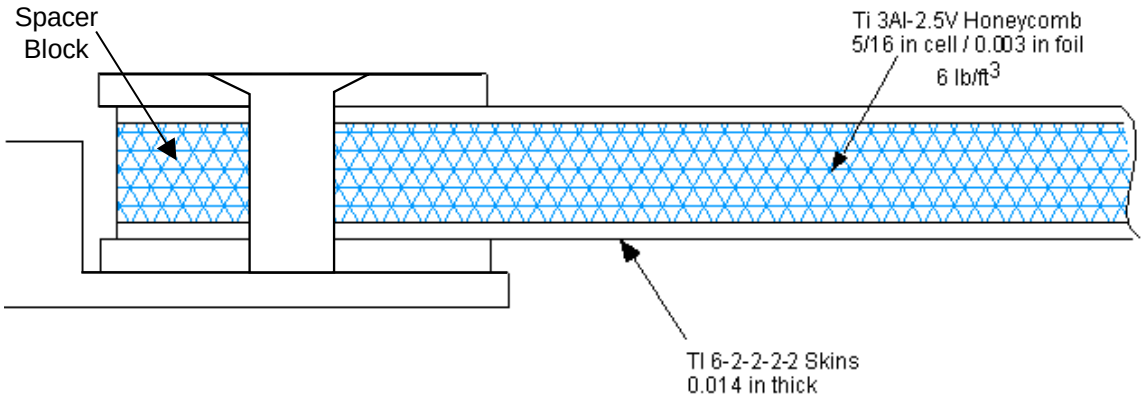

Figure 18 ASTECH Core panel

Table 3 Summary of modal frequencies

Description	Analysis with Pinned Boundary	Test	Analysis with Clamped Boundary
1-1	400	462	587
1-2	828	930	1115
2-1	828	955	1115
2-2	1254	1400	1553

After the modal test was complete, a strain survey was performed on the panel. The acoustic level was increased in steps and the panel strain response was measured at each step. The nominal overall sound pressure levels steps were 142, 146, 154, 160, and 165 dB. The measured narrow-band acoustic spectra used for the strain survey are shown in Figure 19. The strain response versus overall acoustic level is shown in Figure 20.

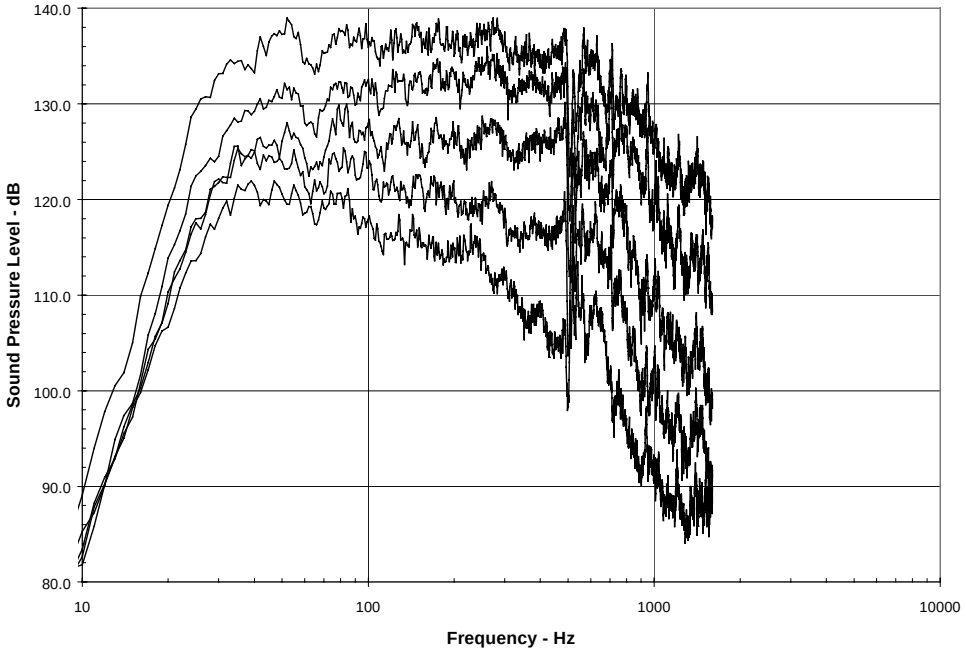

Figure 19 Strain Survey Measured Acoustic Levels

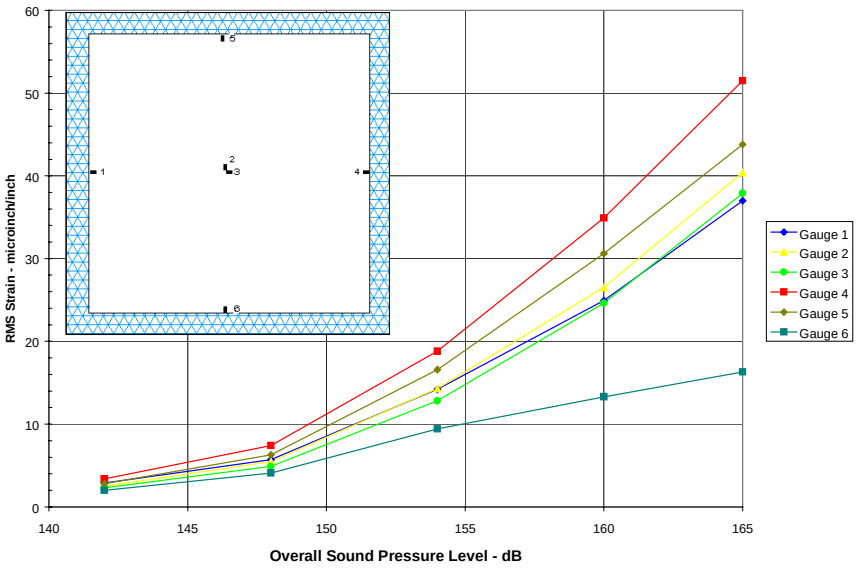

Figure 20 ASTECH Panel Strain Survey Response

During the specimen fatigue portion of the test, the panel was exposed to an overall sound pressure level of 168 dB for 12.5 hours at room temperature. A measured spectrum is shown in Figure 21. The exposure at 168 dB is equivalent to one lifetime of exposure for a 60,000 hour aircraft life on the strake (158dB for 15,000 hours) using a response time compression exponent of 6.5. During the test, there were no signs of structural degradation noticed while monitoring the frequency response of the panel. Periodic ultrasonic non-destructive inspections performed prior to, during, and after the test revealed no damage to the panel.

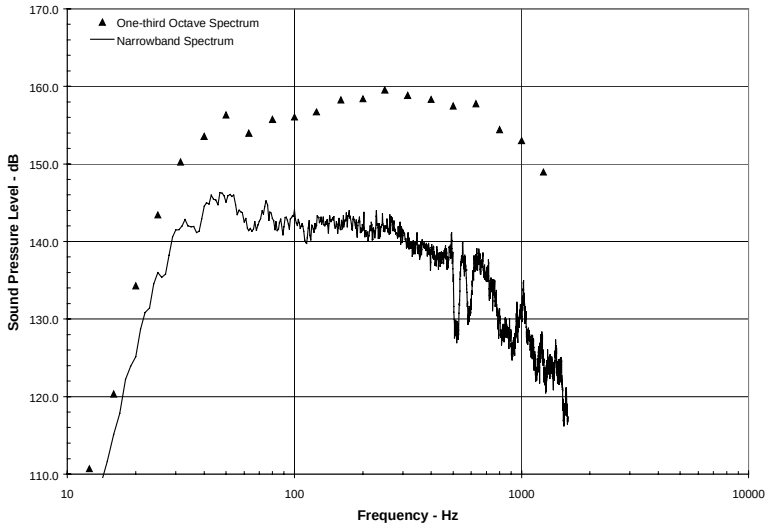

Figure 21 ASTECH Panel Fatigue Spectrum

Polymer Matrix Composite (PMC) Skin / Ti Honeycomb Panel

The second panel was a 1.0 inch titanium honeycomb core panel with 0.042 inch thick quasi-isotropic IM7-PETI-5 facesheets. This structure was produced by laying up the face sheets, and secondarily bonding the face sheets to the titanium core. A sketch showing the cross section of the panel is shown in Figure 22. A finite element model was prepared to predict the modal frequencies of the panel to assure that it was within the testable range of the facility. The analytical model was run with two different edge conditions to provide bounds on the frequency. The analysis predicted the panel frequencies to be about the same as the ASTECH panel. A modal test was performed on the panel installed in the wall of the chamber.

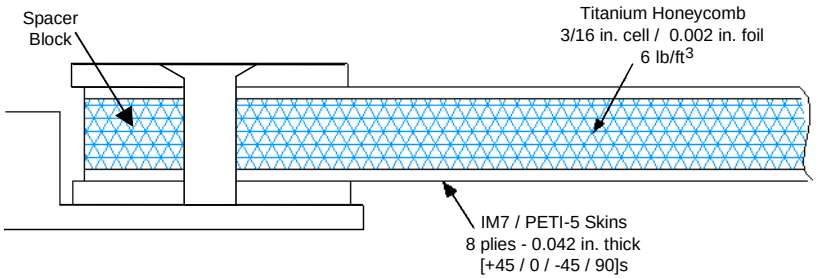

Figure 22 PMC Honeycomb Panel

After the modal test was complete, a strain survey was performed on the panel. The acoustic level was increased in steps and the panel strain response was measured at each step. The nominal overall sound pressure levels steps were 142, 146, 154, 160, 166, and 169 dB. The narrow-band acoustic spectrum used for the strain survey is the same as that used for the ASTECH panel (Figure 19). The strain response versus overall acoustic level is shown in Figure 23.

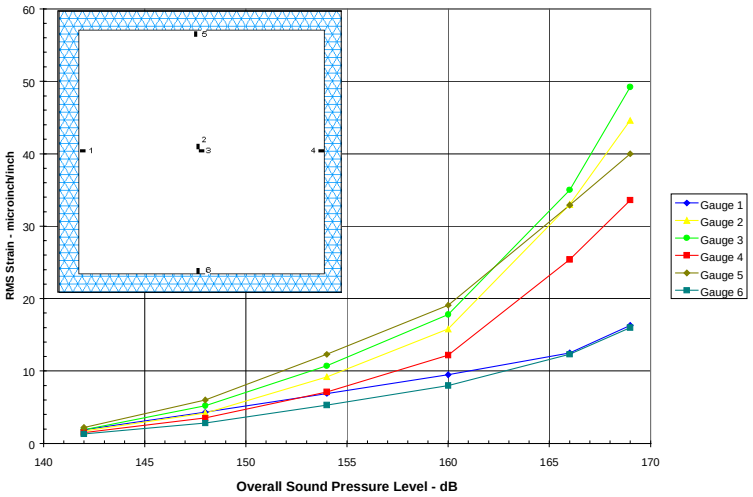

Figure 23 PMC Honeycomb Panel Strain Survey Response

During the fatigue test portion of the test, the panel was exposed to an overall sound pressure level of 166 dB for 4 hours. This is equivalent to one lifetime of exposure on the strake (158 dB for 15,000 hours) using a response time compression exponent of 9.0. During the test, there were no signs of structural degradation noticed while monitoring the frequency response of the panel. Periodic ultrasonic non-destructive inspections performed prior to, during, and after the test revealed no damage to the panel.

Prior plans were to test a second panel with slightly thicker 0.060 inch facesheets. Since no failures occurred in the panel with 0.042 inch facesheets, this acoustic test was abandoned. A third panel with the 0.042 inch facesheets was also to be tested at 350 °F. Since the original panel with the 0.042 inch facesheets performed so well in the fatigue test, it was used to test an additional equivalent lifetime at 350 °F. The panel was simultaneously exposed to 350 °F on the face and an overall sound pressure level of 164.5 dB for 18 hours.

No failures were detected as a result of this testing. Because of the small size of the panels compared to actual aircraft skins, yielding high panel frequencies, and the drop in input acoustic energy above 500 Hz, the strain levels measured are quite low. Therefore, the fact that the panels survived this test is not evidence that PMC honeycomb skins will last the life of the aircraft. Fatigue testing of PMC honeycomb specimens on a shaker was used to determine strain levels required for failures and to characterize the failure mechanism as described below.

Sonic Fatigue Coupon Testing

The primary step to determining the acoustic fatigue life of candidate structures is to calculate the damage caused by panel strain response. Sonic fatigue coupon tests were conducted on candidate materials that were to be used in the skin stringer structural concepts. Ti 6-2-2-2-2 and IM7/PETI-5 were the primary material candidates that had been previously tested by the HSR CAS and Metals ITD teams under the material development phase of the program. The purpose of these tests was to study the effect of static pre-load and temperature on fatigue life. The results of these tests were then to be used in the design and evaluation of candidate structures. Midway through the testing in 1997, metals were abandoned as candidates for the aircraft skin.

Test Approach

Flat specimens, in the basic shape shown in Figure 24, are cut from sheet stock between 0.050 and 0.070 inches thick using a water jet cutter. A strain gauge is located on the specimen at the location of maximum strain for the second bending mode, as indicated by finite element analysis and initial testing. The failures occur in the narrow, straight section where no stress concentration factor exists. An optimization technique is used for specimen design that constrains the frequency of the specimen to be between 400 and 600 Hz, and assures that the failure occurs at the strain gauge location. An amplifier beam may be used to increase the input level into the test beam for some materials so that higher strain levels can be achieved.

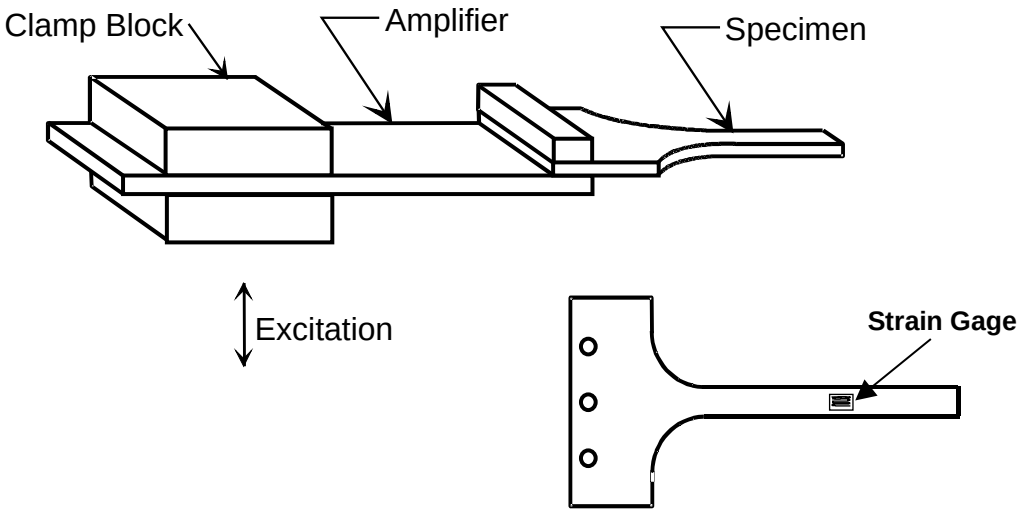

Figure 24 Second Bending High Cycle Fatigue Specimen

The “R” factor is defined as the ratio of the minimum to maximum applied cyclic load. R = -1 represents a zero mean stress and completely reversed bending typical of response to sonic excitation. For testing at R not equal to -1, the specimens may be preloaded, as shown in Figure 25, with a static bending strain via a trapeze located at the node line of the second bending mode shape. Loading at the node line reduces the effect of the pre-load on the dynamic characteristics of the beam. Up to four specimens at a time are attached to the shaker and vibrated with a narrow band random input centered on the second mode. Each specimen is computer monitored to track the frequency and strain level, and to terminate the test if the frequency changes by 10%.

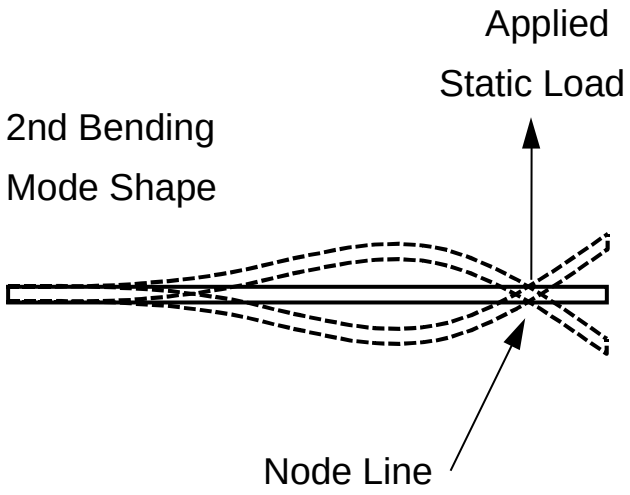

Figure 25 Static Load Application

Characterization of the Data

For the fatigue data presented, a least squares curve fit of the form $\log(\varepsilon)=a[\log(N)]^b$, where *a* and *b* are constants, has been calculated. Coefficients a and b are shown in the figures which present ε-N data. In many cases, the number of data samples available to create this are minimal, causing the potential error in the curve fit to be large.

Titanium 6Al-4V Testing

Twenty annealed Ti 6Al-4V specimens were high cycle fatigue tested during September and October 1995. Testing was conducted at room temperature with a zero mean stress condition (R=-1), representing completely reversed bending, and stress concentration Kt = 1.0. Measured data points and the least squares curve fit are shown in Figure 26.

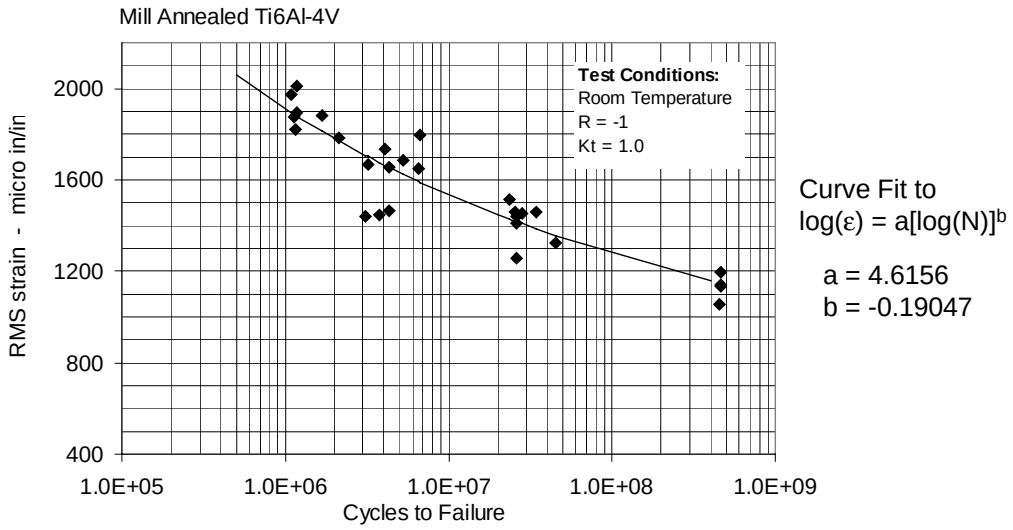

Figure 26 Random Bending Fatigue Data for Annealed Ti 6Al-4V

Titanium 6-2-2-2-2 Testing

Ten baseline specimens of this material in the solution treated and aged (STA) condition were tested without pre-load strain in 1997 to compare with the material tested previously. Six specimens were tested with the mean strain equal to one-third of the rms strain (R=-1/2), and five specimens were tested with the mean strain equal to the rms strain (R=0). Previous testing showed that an increase in temperature to 350 degrees F is of no consequence for titanium 6-2-2-2-2, so specimens were tested at room temperature only.

Results from the tests are presented in Figure 27. The baseline specimens that were tested without a pre-load, matched the data measured in previous tests well. Both sets of data, as well as a least squares curve fit for the no pre-load data are presented. The preloaded specimens failed with considerably more scatter, but trends can still be observed. The R=-1/2 data is fairly close to the no pre-load data, and the R=0 data falls mainly below the no pre-load data. The second solid curve at the bottom is a Goodman

equation modification of the no pre-load least squares curve fit. The fatigue data for R=0 pre-load falls above this reference curve. For comparison, the least square curve fit for annealed Ti 6Al-4V from Figure 26 is also shown (as a dashed line). The endurance limit for Ti 6-2-2-2-2 is considerably higher than that for annealed Ti 6Al-4V.

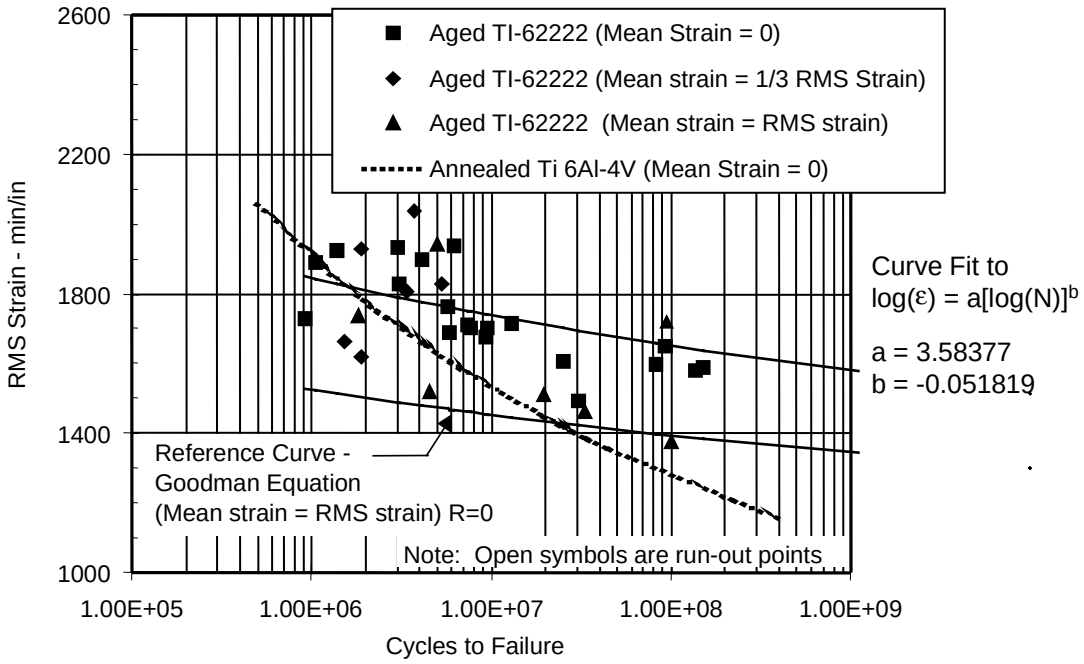

Figure 27 Random Bending Fatigue Data for Aged TI 6-2-2-2-2

IM7/PETI-5 Testing

Sonic fatigue criteria for metal structure is often based on stress vs. number of cycles to failure (S-N). For composites, a maximum limit rms strain or endurance strain is defined and panels are designed not to exceed this limit. Coupon and beam tests were conducted on IM7/PETI-5 samples to measure strain and the number of cycles achieved at failure. Coupon testing was conducted at ambient conditions and at elevated temperature (350^{o}F) without pre-load. The standard method for pre-loading these specimens, i.e. a trapeze mechanism, was attempted but was unsuccessful because (a) the IM7-PETI-5 material is rougher and quickly wore through the pre-loading mechanism and (b) the specimens were sufficiently flexible that too great a deflection was required.

Representative joints were tested in the beam tests. The joint specimens consisted of two different lay-ups so the strain allowable is somewhat insensitive to lay-up directions. The results of these tests are summarized in Figure 28. It took very high strains, on the order of 2400 μinches/inch and above, to get the material to fail.

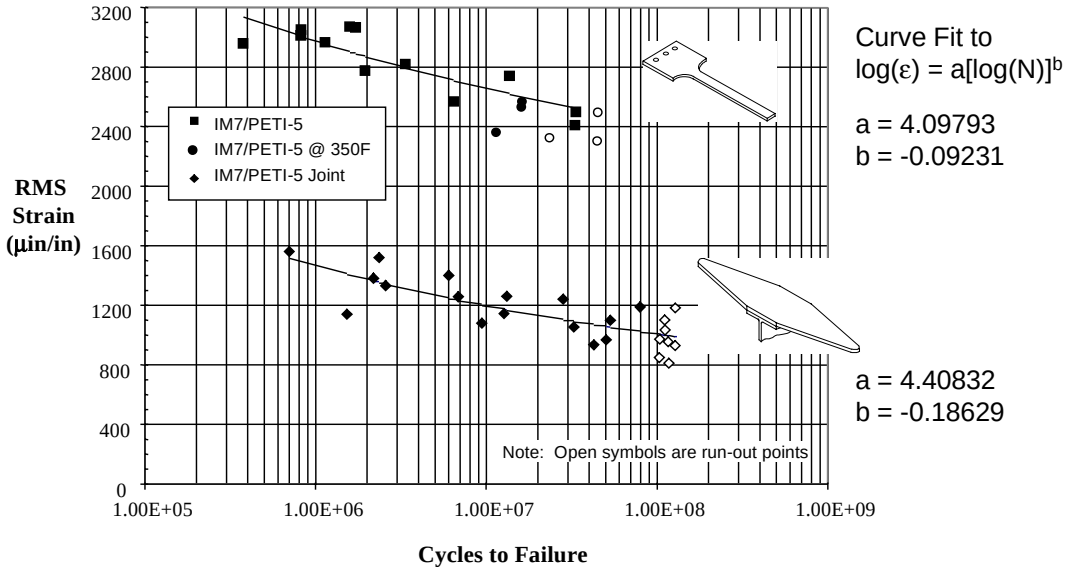

Figure 28 Random Bending Fatigue Data for IM7/PETI-5

As indicated, the effect of joint configuration is a primary factor in the capability of a structural component. Representative joints were tested as shown in Figure 29. From the results shown in Figure 28, the 800 μin/in allowable strain for the joint specimen is a factor of three lower than that for the parent material. The joint test specimen was configured to represent skin/stringer joints and the test allowable is appropriate for this type of fuselage component. The lower allowable results from the very high stress concentration at the edge of the stringer flange, leading to a failure mechanism characterized by de-bonding of the flange from the skin plies. Some reinforcement at this edge, such as lapping several outer plies further onto the skin panel, would substantially increase the fatigue capability of this configuration.

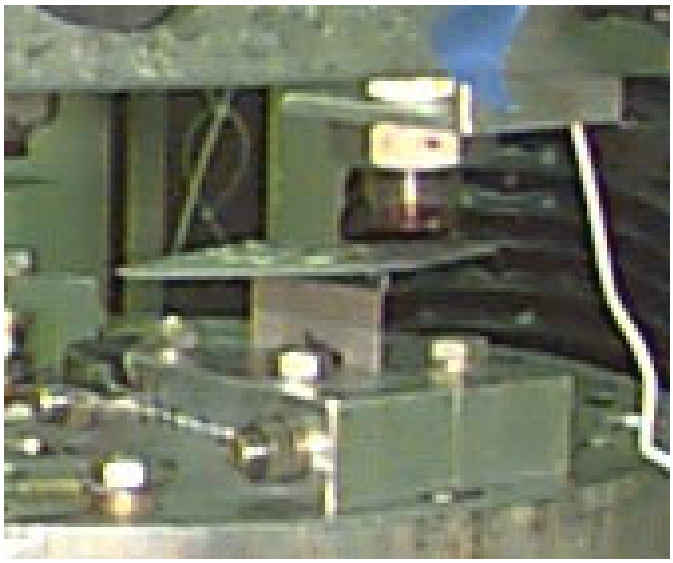

Figure 29 Representative Joint Specimen in Test

Additional High Cycle Fatigue Testing

Although Ti 6-2-2-2-2 and IM7/PETI-5 testing is of primary interest, several other metal and composite materials were characterized during the HSR sonic fatigue program. Table 4 summarizes high cycle fatigue tests and references figures that present test data. Unfortunately, efforts to obtain TiGr material for coupon testing were unsuccessful.

Table 4 HSR High Cycle Fatigue Test Summary

MATERIAL	CONDITION	TEST DATE	COMMENTS	FIGURE
Metals				
Ti 6AL-4V	Annealed	Sept. 95	Room temp., R=-1, Kt=1.0	Fig.26
Ti 6-2-2-2-2	SPF Disbond	Oct. 95		
	Annealed, Aged, Pickled,	Sept. 94 - July 97	Room temp., 350^{o}F, no preload, R = -1, R=-1/2, R=0	Fig. 27
SP 700	Annealed, Sim SPF & Aged	July 95, Nov. 95		Fig. 30
IMI 550	Annealed, Sim SPF & Aged	June 95, Nov. 95		Fig. 31
β–21s	STA	Sept. 95	Room temp, 350^{o}F	Fig. 32
Composites				
IM7/K3B	includes HYBOR, Hybrid	Nov. 95	Room temp, 350^{o}F	Fig. 33 Fig. 34
IM7/PETI-5	includes 25% Boron, 10% Boron	Feb. 96, Apr. 96, Sept. 97	Room temp, 350^{o}F	Fig. 28

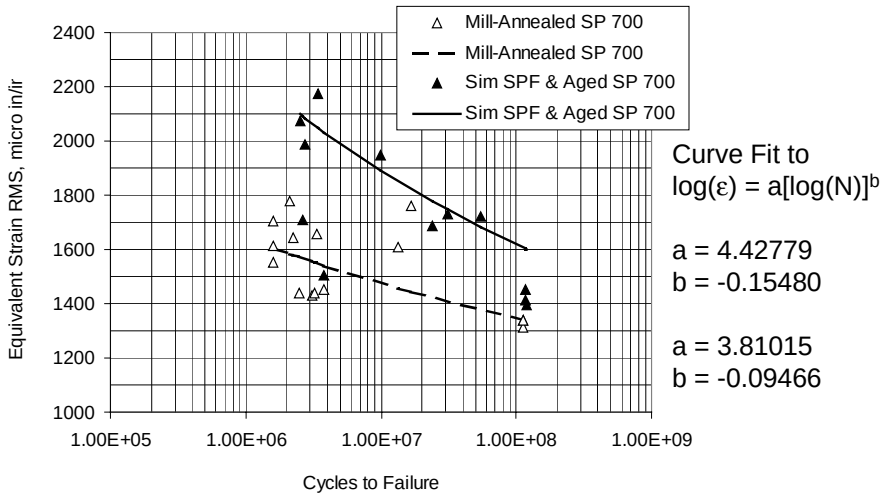

Figure 30 Fatigue Data for SP 700

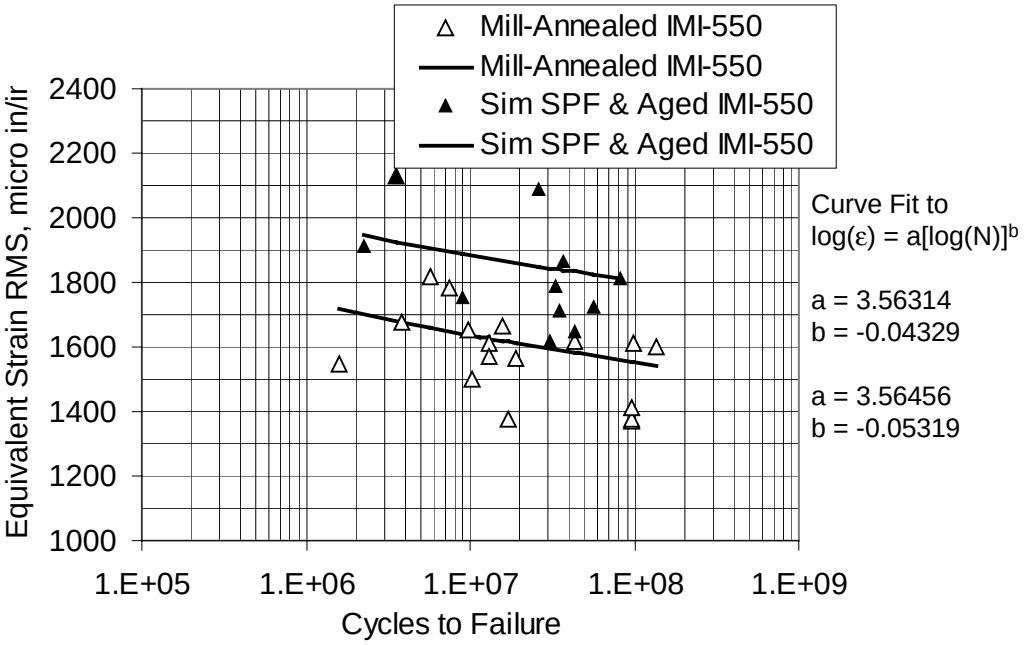

Figure 31 Fatigue Data for IMI 550

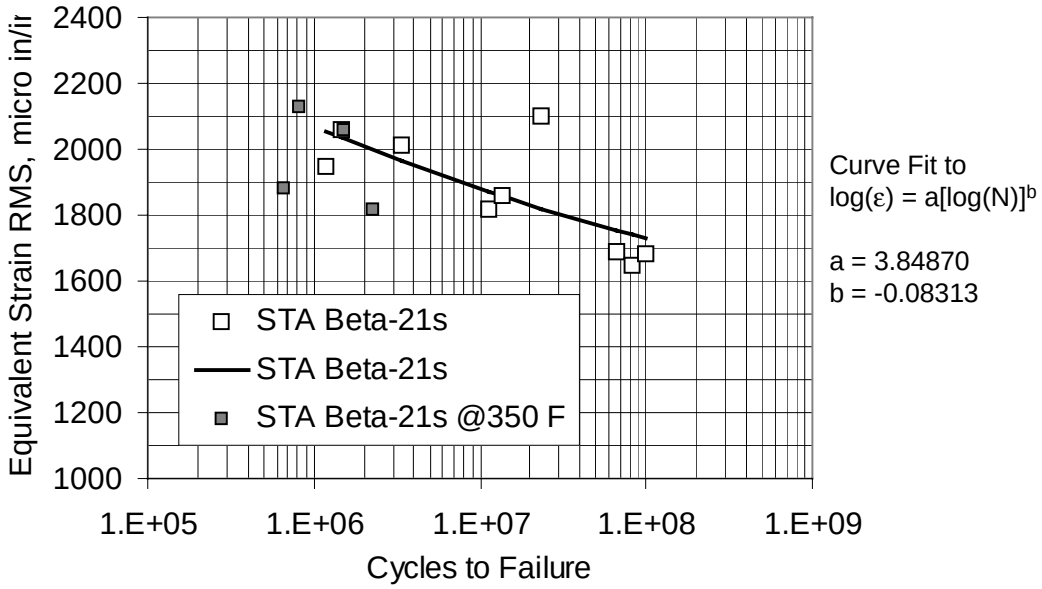

Figure 32 Fatigue Data for β–21s

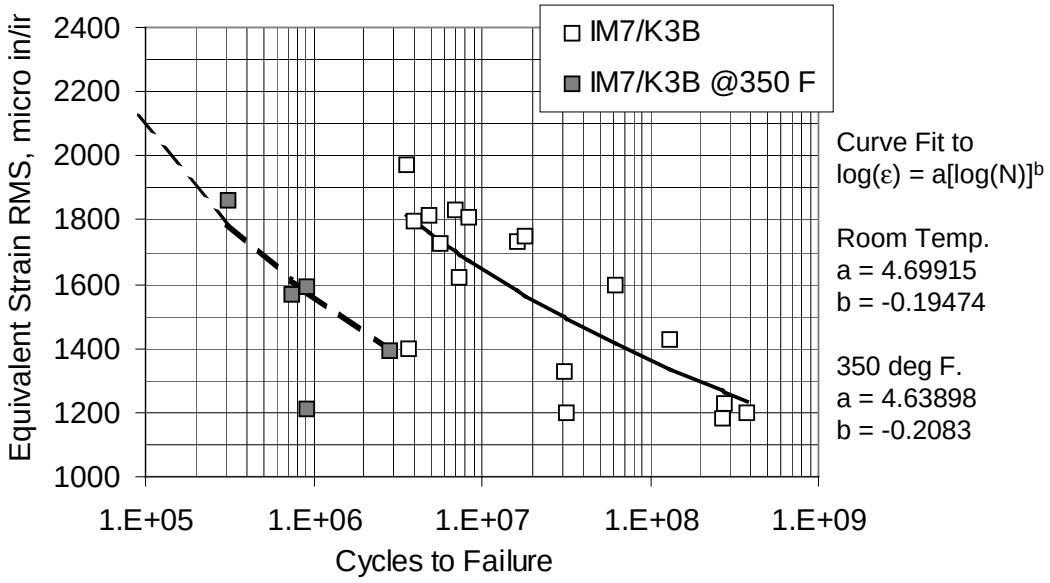

Figure 33 Fatigue Data for IM7/K3B (RT and 350°F)

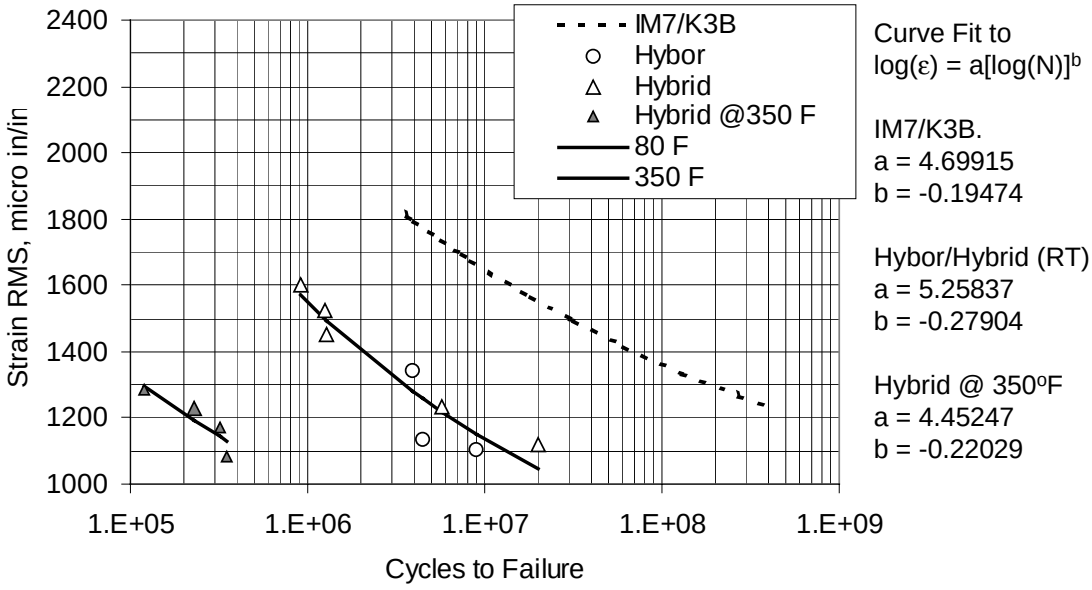

Figure 34 Fatigue Data for IM7/K3B, HYBOR, & Hybrid

Material Characterization for Sonic Fatigue Analyses

Skin/Stringer Structural Concept

The IM7/PETI-5 test data (Figure 28) was utilized to characterize HSCT fuselage skin/stringer structure. A limit strain value is selected from test data, including the effects of temperature, appropriate joint configuration, and "R" factor. The effect of elevated temperature on coupon test results was a slight reduction in allowable strain. The importance of testing representative joint configurations rather than coupons alone is evident from the test data. Joint specimen strain values for failure at a specific number of cycles were approximately half or less than those for beam specimens. The "R" factor is defined as the ratio of the minimum to maximum applied cyclic load. The tested value of R = -1 represents a zero mean stress and completely reversed bending typical of response to sonic excitation. Based on beam and joint specimen tests and the long life requirement of over 10,000,000 cycles for the structure, a value of 800 μin/in is used as the allowable RMS strain in any component of the skin-stringer system.

Selection of the appropriate limit endurance strain is a primary factor in defining required panel and substructure geometry for a sonic fatigue resistant design. For example, the required thickness of a flat rectangular panel clamped on all edges is related to the allowable mean strain ε_{allow} by the equation:

$$\text{minimum thickness} = C \left(\varepsilon_{allow} \right)^{-b}$$

where: C = Proportionality constant
b = Coefficient based on type of material
0.5 for isotropic materials (metals)
0.667 for composites, after Jacobson [ref. e]
0.75 for laminate composites, after Holehouse [ref. f]

Regardless of the values of C and/or b, a 50 percent reduction in the allowable strain can result in a 40 to 70 percent increase in the minimum required thickness as shown in Figure 35. This example is used only to illustrate the implication of selecting the proper value for limit strain and the actual values in this example are not relevant to development of HSR sonic fatigue design guidelines. Based on relevant test data, 800 μin/in is selected as the appropriate design value for limit endurance strain.

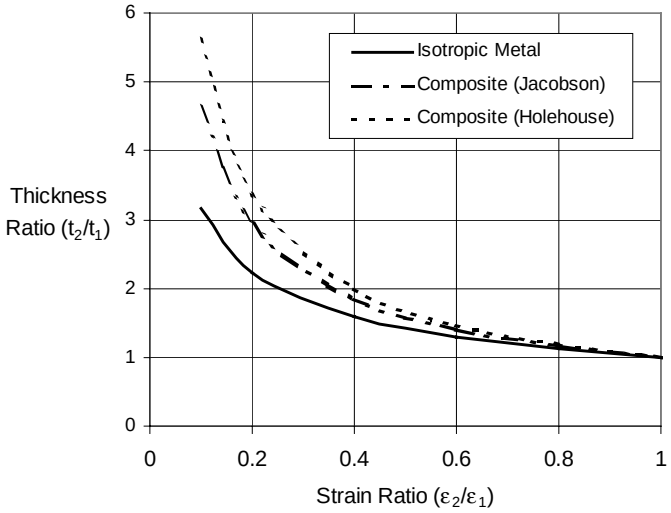

Figure 35 Relationship of Thickness To Strain for Clamped Rectangular Panels

PMC-TI Honeycomb Structural Concept

As indicated, acoustic tests of honeycomb panels did not induce failures. Preliminary high cycle vibration tests were conducted on 30 inch by 2 inch PMC-TI honeycomb beams to measure strain and the number of cycles achieved at failure. The beams were strips cut from test panels and were previously used as spacer blocks in acoustic tests (Figure 22). The test beam core was 1 inch honeycomb composed of 3/16 inch cells of 0.002 inch foil. IM7/PETI-5 face sheets were 0.042 inches thick, consisting of eight 0.0052 inch $[45/0/-45/90]_S$ plies. The test setup and results of these limited tests are shown in Figure 36. Results are shown as data points and a solid curve fitted to those points. For comparison, results for IM7/PETI-5 representative joint tests previously discussed and shown in Figure 28 are also plotted (dashed curve). During testing, cohesive bond failure occurred near the ends of the beam, as shown in Figure 37, due to shear stress in the adhesive layer.

A NASTRAN model of the test beam strip was generated to validate the analysis material parameters to be used in development of design curves for panel structure. Random vibration response analysis was performed on the model of the beam fatigue test configuration with base excitation of the flexures supporting the ends of the beam strip. The analytic RMS strain and spectral results at the center of the beam correlate with test data as shown in Figure 38. Based on test results, failure criteria for PMC-TI honeycomb panel structure are based on shear stress near the interface of the panel and substructure frames and on axial strain at the center of the panel. 800 μin/in was selected as the appropriate allowable strain for honeycomb panel sonic fatigue analyses.

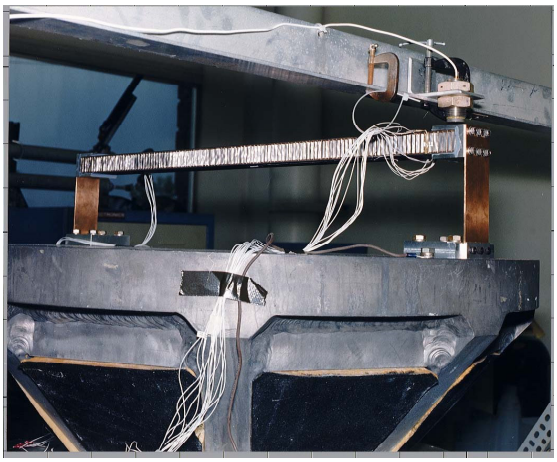

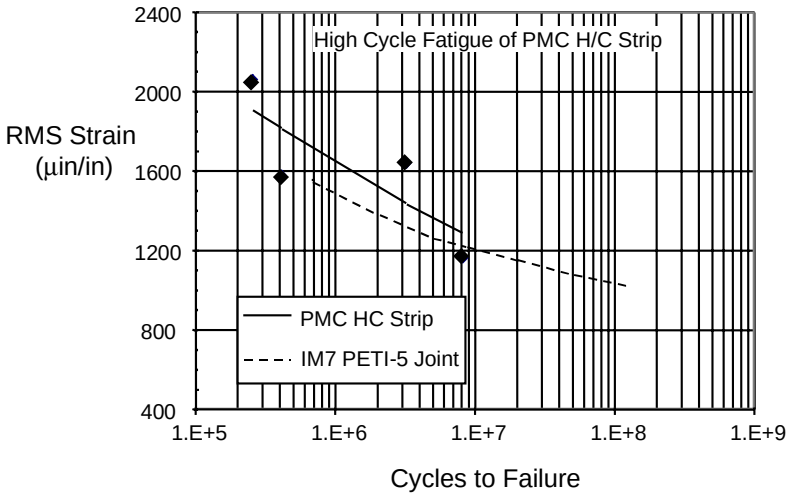

Figure 36 Material Characterization of PMC-TI Honeycomb

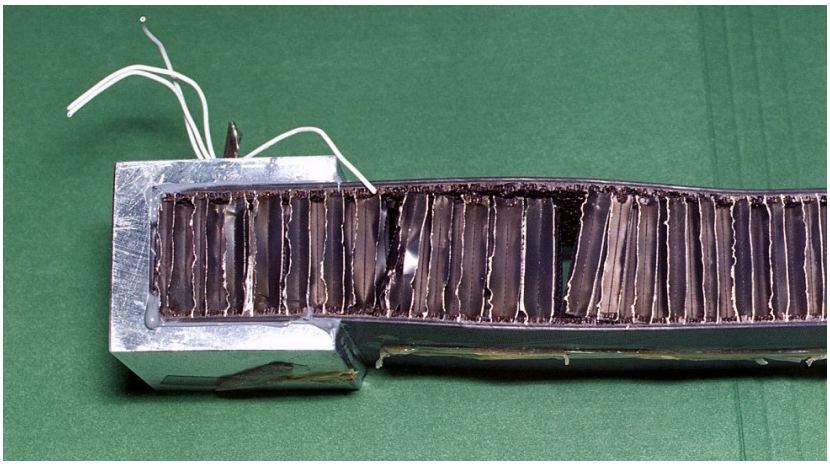

Figure 37 PMC-Ti Honeycomb Strip Failure

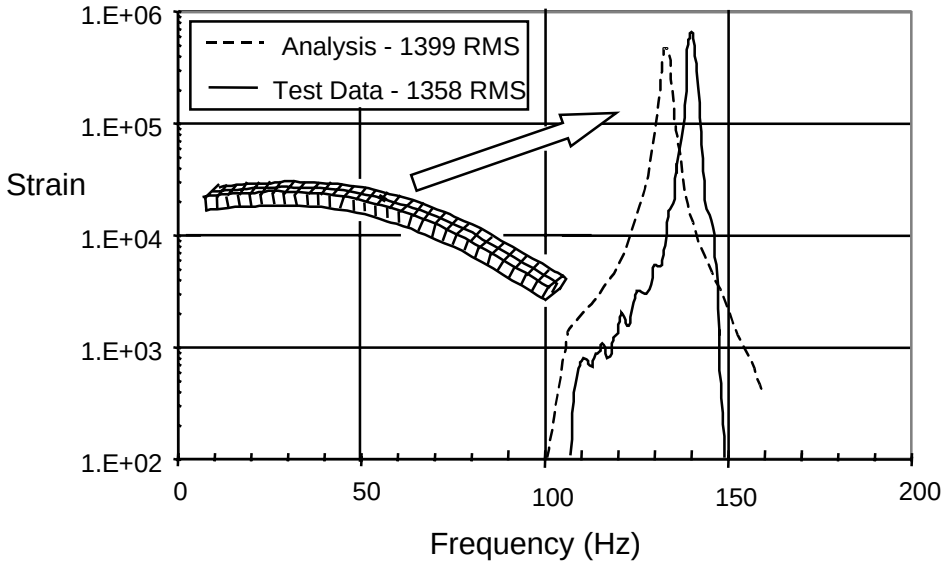

Figure 38 Analysis-Test Comparison for Honeycomb Beam

4.0 SONIC FATIGUE ANALYSIS TECHNIQUES

High acoustic transmission may occur in aircraft skin structure subjected to high acoustic noise from various sources, such as aerodynamic flow, engine inlet and exhaust noise. Minimization of the thickness of skin panels and substructure has the potential for significant weight savings over an entire aircraft. The objective of this task was to develop analysis techniques to accurately predict response of airframe skin and substructure to sonic fatigue loading.

Sonic Fatigue Structural Response Code Development

The non-linear random structural response NASTRAN Direct Matrix Abstraction Programming (DMAP) code developed by NASA was chosen as the best base application for sonic fatigue analysis. This development proceeded through 1998 with the goal to employ it for sonic fatigue analysis of baseline HSCT structure when the process sufficiently matured. This was not accomplished to date but code development should be completed as a basis for more accurate sonic fatigue analyses to fulfill the needs of other programs. Efforts related to this non-linear code development are reported here as are descriptions of the preliminary analysis tools used and the results of these studies.

NASTRAN DMAP / nCode Fatigue Module

To validate the DMAP, a clamped aluminum panel test case was run in 1997 (Figure 39) and the results matched well with previous analysis methods.

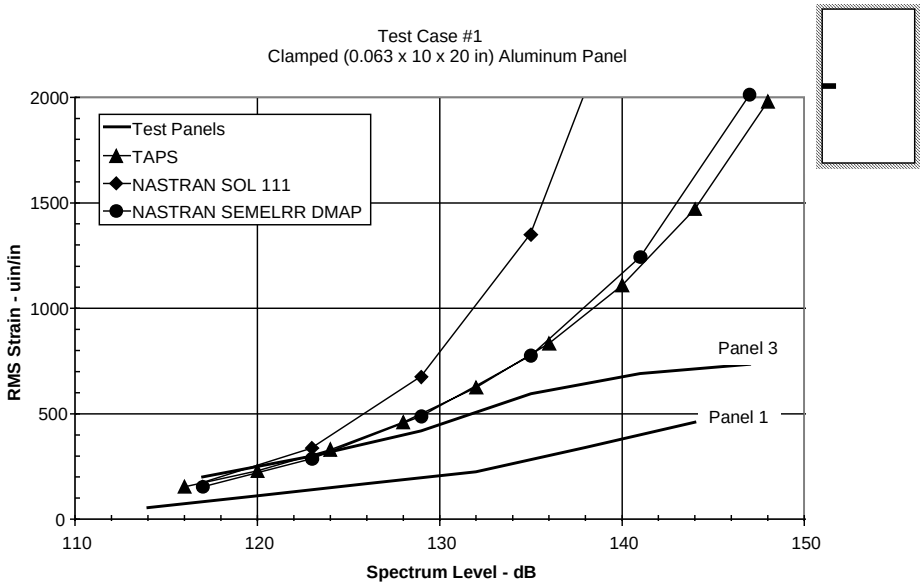

Figure 39 Clamped Aluminum Panel Test Case

Once the panel response has been determined, it is necessary to perform the fatigue life calculation for the structure. Methods were examined to calculate the fatigue life. A fatigue module that can be purchased through MSC will produce life contours based on panel response and material properties. This would provide a seamless method for performing sonic fatigue analysis based on commercial software which does not depend on HSR personnel for maintenance/support because MacNeal Schwendler plans to incorporate this software into their FATIGUE module. The company that currently supports this module, nCode international, was contacted to see how to get output from the DMAP and project fatigue data into this module. A test case was prepared to see how well the DMAP and fatigue module worked together to predict the failure time, and would allow nCode an opportunity to evaluate our needs. The test case involved vibration testing a cantilevered beam with excitation in the first two modes. The beam had strain gauges installed at the locations shown in Figure 40 and was run until a failure occurred. The two beams tested both failed near the root gauge with the response and failure times summarized in Table 5.

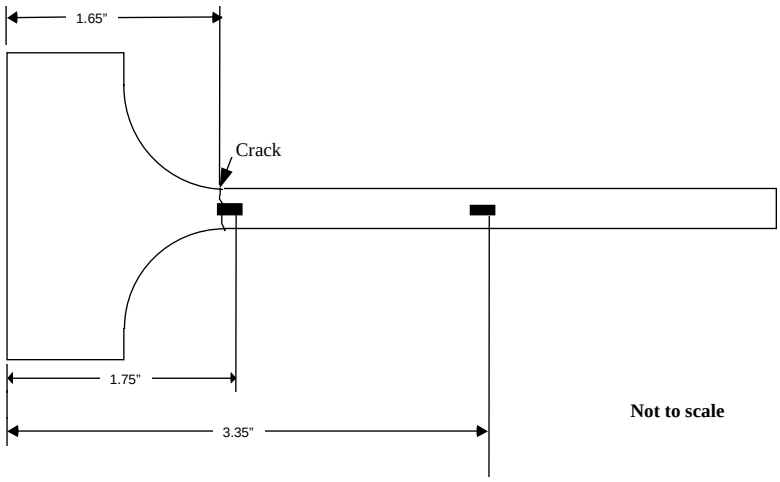

Figure 40 nCode Beam Test Specimen

Table 5 nCode Beam Test Summary

Specimen	**Level**	**Input Acceleration** (g's rms)	**Root Strain** (uin/in rms)	**Mid Strain** (uin/in rms)	**Time to Failure** (hrs:min:sec)
Beam 2	-9dB down	11.2	1140	579	—
Beam 3	-9dB down	11.3	1002	525	—
Beam 2	0 dB	31.5	—	1340	0:42:51
Beam 3	0 dB	31.79	1861	1351	0:33:50

DMAP response estimations have not matched the beam response during the test very well. Since the beam has a free edge, it exhibits fairly linear behavior even at very high displacements. This may be the reason why the non-linear DMAP does not estimate the response very well.

In addition to the nCode process, an alternate was selected which involves writing code to calculate the life of the structure. The code would read the response results from the DMAP and fatigue data from a database and calculate the fatigue life. The two methods are shown in Figure 41. Database and code development has not been completed. The linear NASTRAN technique described below was used as an interim approximation of sonic fatigue response.

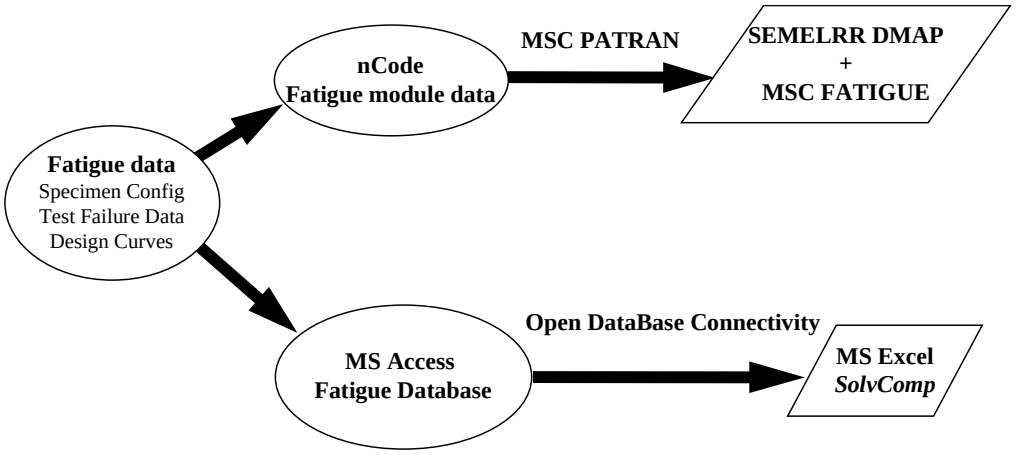

Figure 41 Material Fatigue Data Processes

Sonic Fatigue Interim Process

The flowchart of Figure 42 compares the interim HSCT sonic fatigue process with the final analysis process discussed above. Although both processes utilize the same basic data - structural design, material fatigue data and the appropriate sonic loading - the planned process would have provided a seamless method for performing accurate sonic fatigue analysis based on commercially maintained and supported software.

The more complex interim process was used for the analyses discussed in Section 5.0. Static and thermal loads are pre-applied to the model using NASTRAN static solutions. The acoustic loads are then applied to the model and RMS stress determined using the linear frequency response solution within NASTRAN. RMS stress contour plots are generated using a post processor (usr_random), provided by MacNeal Schwendler (MSC) and PATRAN. RMS strain levels are determined by loading stress data obtained from the post processor into Microsoft EXCEL and computing strains. The strain values are then compared with the material strain endurance limit to determine the adequacy of the structural design. Parametric analyses using this interim process were utilized to develop HSCT sonic fatigue design curves.

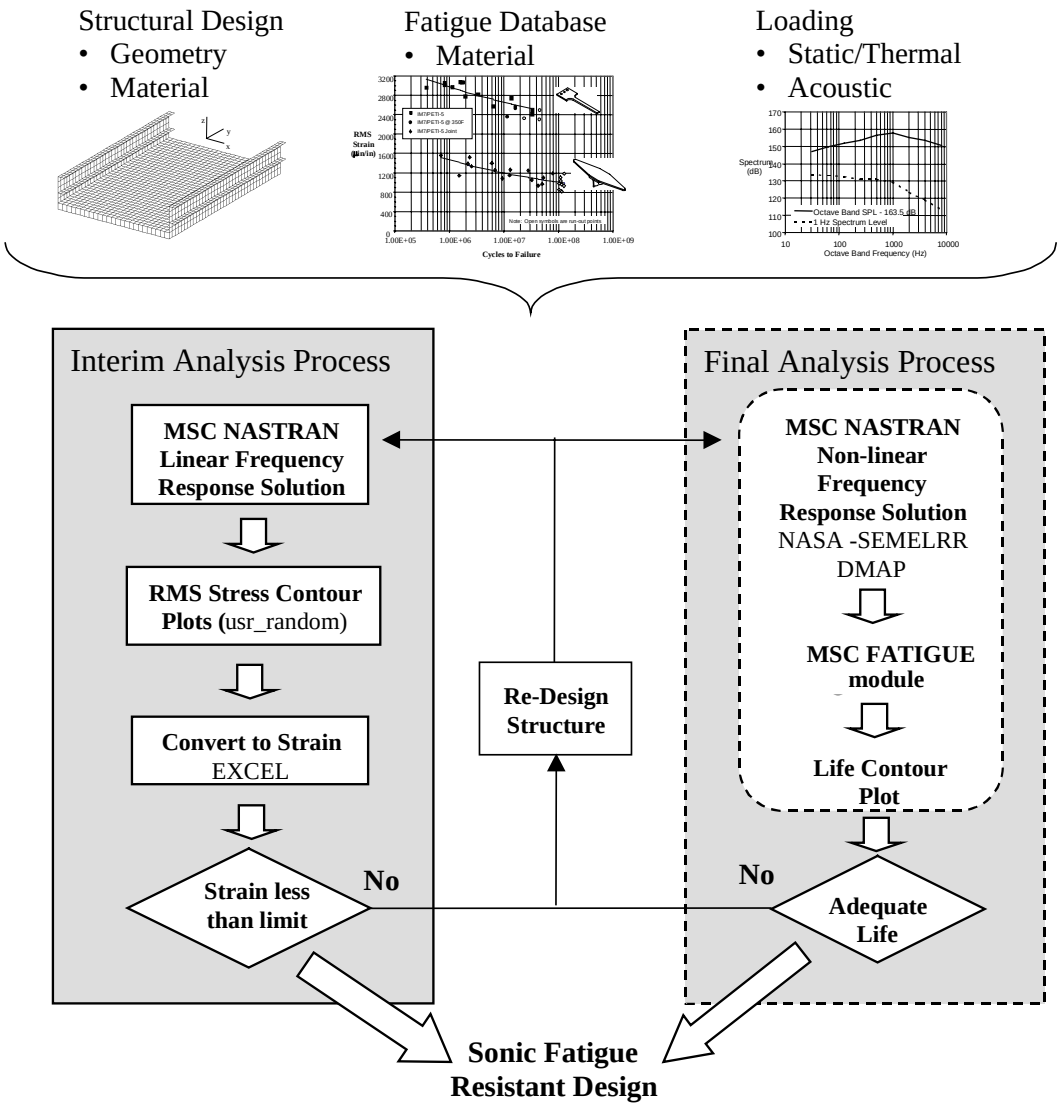

Figure 42 Sonic Fatigue Analysis Interim and Final Processes

5.0 SONIC FATIGUE DESIGN REQUIREMENTS

Minimization of the thickness of skin panels and substructure has the potential for significant weight savings over an entire aircraft. The objective of this task was to develop guidelines for initial design of efficient fuselage structure tolerant of the severe exterior acoustic noise environment experienced by the High Speed Civil Transport (HSCT). Sonic fatigue analyses were conducted on representative HSCT side fuselage skin panel/stringer/frame and honeycomb panel/frame sub-components to define structure with acceptable sonic fatigue life (60,000 hours times a scatter factor of 2) when subjected to the sonic fatigue design load including a 3.5 dB factor of safety.

Skin/Stringer Development

Two alternate structural systems are being studied for HSCT fuselage structure. The first of these is a system of IM7/PETI-5 composite panels stiffened by a grid consisting of longitudinal frames and web stringers between those frames. Sonic fatigue design curves were developed for this configuration.

Panel Geometry

For simplicity, the slightly curved HSCT skin structure was approximated as a flat panel and substructure system since the fuselage side between windows and floor, where acoustic levels are highest, is practically flat. The three-bay NASTRAN model (Figure 43) consisted of three adjacent skin panels bordered by four longitudinal stringers and two frames. Stringers were represented by webs normal to the panels and flanges or tear straps attaching the stringer to the panel. The skin and substructure concept analyzed is representative of that used in the HSCT fuselage conceptual design. Design curves are intended to provide the minimum required thickness of the skin (t_{skin}), stringer web ($t_{stringer}$) and tear strap area ($t_{tear\ strap}$) for a given distance between stringers (a), length (b) and height (h) of stringers. The tear strap thickness includes both the stringer flange and the panel itself. Composite IM7/PETI-5 rectangular panels with short side dimensions (a) of 6.0 to 12.0 inches between stringers and aspect ratios (b/a) of 1.0 to 4.0 were studied to provide design curves.

Analysis Procedure

The interim analysis process shown in Figure 42 was employed. Prior to NASTRAN parametric analyses, initial geometric sizing was performed by traditional sonic fatigue methods for simple panels. The analytic prediction criteria included these assumptions:

- The temperature over the surface of a panel, 350^{o}F, is uniform. Temperature stabilization between the panel surface and substructure occurs rapidly negating

unreasonably high thermal stresses. Thermal effects are accounted for in the limit strain estimation.

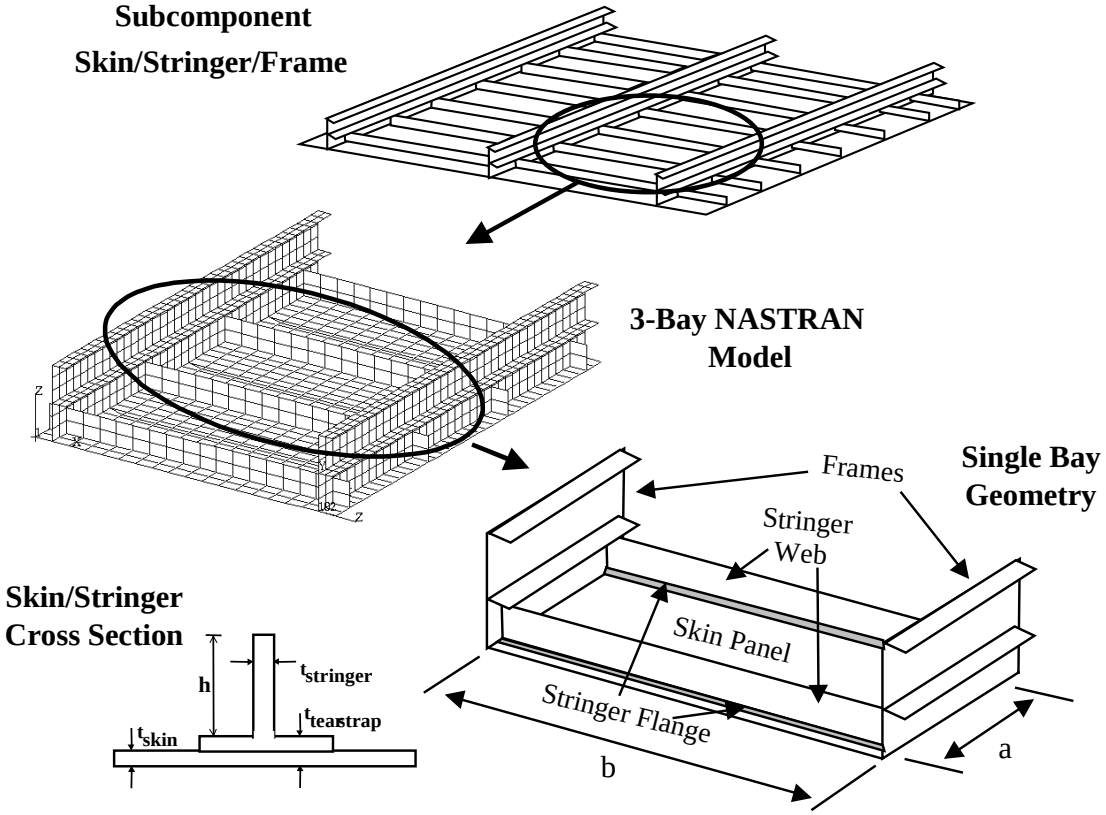

Figure 43 HSCT Fuselage Skin/Stringer Model

- The excitation is random amplitude broadband noise.
- The dominant and damaging structural response of the skin panel occurs at its fundamental mode frequency.
- Highest strain occurs if the model edges are assumed clamped.
- Curvature generally greatly enhances the fatigue life of panels. For conservatism, flat panels were analyzed.
- A mean damping value of 0.01 is used in the absence of definitive test data for a particular configuration.

Three sets of design curves were developed, defining the minimum thickness requirements for the skin, stringer web, and stringer flange. The Boeing Composite Panel Sonic Fatigue Design Tool (SolvComp), was utilized initially to size skin panels. This application, developed for unstiffened panels, implements the following steps:

(a) Identify the panel to be analyzed (basic geometry, curvature, material, damping)
(b) Assume a thickness

(c) Compute the panel fundamental frequency (assuming clamped edges)
(d) Estimate the noise spectrum level at the resonant frequency
(e) Calculate the rms strain by the Jacobson method [Reference e] and compare the calculated value with the limit strain value
(f) Iterate until the panel thickness is consistent with the limit strain.

Figure 44 is a sample output from the SolvComp spreadsheet.

Noise Type	a	b	t	R	ρ	ζ	Dxx	Dxy	Dyy	Dzz	Freq Flat	OASPL + 3.5	Spectrum Level	Time @ cond	# cycles	RMS Strain (Jacobson)
	in	in	in	in, 150 max	lb/in^3	C/Cc	lb-in	lb-in	lb-in	lb-in	Hz	dB	dB	hours		µin/in
Exhaust	8.3	10.2	0.080	70	0.058	0.010	456.0	148.0	387.0	159.0	425	163.5	131.1	60000.0	9.2E+10	636
Exhaust	8.0	8.0	0.057	70	0.058	0.010	164.1	53.3	139.2	57.2	383	163.5	131.1	60000.0	8.3E+10	800
Exhaust	8.0	16.0	0.081	70	0.058	0.010	479.3	155.6	406.7	167.1	383	163.5	131.1	60000.0	8.3E+10	800
Exhaust	10.0	10.0	0.066	70	0.058	0.010	251.1	81.5	213.1	87.6	282	163.5	131.0	60000.0	6.1E+10	800
Exhaust	10.0	20.0	0.094	70	0.058	0.010	733.5	238.1	622.5	255.8	282	163.5	131.0	60000.0	6.1E+10	800
Exhaust	12.0	12.0	0.074	70	0.058	0.010	361.6	117.4	306.9	126.1	221	163.5	131.0	60000.0	4.8E+10	800
Exhaust	12.0	24.0	0.106	70	0.058	0.010	1056.3	342.8	896.5	368.3	221	163.5	131.0	60000.0	4.8E+10	800

Figure 44 Sample of SolvComp Sonic Fatigue Computation

Parametric NASTRAN linear acoustic response analyses were then conducted on the three bay model of Figure 43 to validate the initial skin panel thickness design curve developed from SolvComp results and to provide results used to develop substructure design curves. Analysis variables were the distance between stringers (a), the distance between frames or length of the stringers (b), the thickness of the skin (t_{skin}), the height of the stringer web (h), the thickness of the stringer web ($t_{stringer}$), the thickness of the tear strap area, including the skin and stringer flange, ($t_{tear\ strap}$) and the frame geometry. The NASTRAN model consisted of 1663 nodes connected by 1598 elements.

The implication of employing linear analysis in the interim process rather than the eventual non-linear final analytic procedure is that, dependent on the characteristics of the structural response, strains may be overestimated for high loading conditions and potentially high response. Linear analysis will result in some degree of conservatism but that degree is unknown. As an example of the potential for conservatism associated with linear analysis, results for a simple clamped aluminum panel [Reference a] are shown in Figure 39. NASTRAN SOL 111 is a linear frequency response solution which is compared to the non-linear DMAP solution. This comparison should not be applied to composite structural systems and is provided only as an illustration of the effect of using linear response results.

Results

Results of the interim sonic fatigue analyses for skin/stringer configurations indicated that:

- strain of the skin was relatively independent of the stringer and frame geometry and was primarily a function of the panel size (a x b). The skin thickness from SolvComp was, therefore, assumed for all NASTRAN analyses. This assumption proved successful.

- frame geometry had little effect on the strain in other components. Frame height of three times the stringer web height was considered representative of aircraft structure. As seen in Figure 43, the frame geometry was an F section. Frame thickness was typically assumed equal to that of the stringer, but no less than 0.1 inch.

Data analyses of multiple SolvComp and NASTRAN results were performed and design curves were developed to limit RMS strain in the skin panels and stringers (web and flange) to 800 μin/in. In these analyses, it was assumed that the stringers are fixed to the frames.

(a) Skin: The required thickness of panels of various sizes were computed for the acoustic fatigue design load and properties of the material by the SolvComp application. Figure 45 is a plot of the results which can be used as a design aid during initial sizing of fuselage panels. 0.125 inch thick panels should be sufficient for panels up to 12 by 48 inches.

(b) Stringer Web: The required minimum thickness of the stringer web is a function of the skin panel thickness and the web aspect ratio - length of stringer (b) divided by the height of the web (h) - as shown in Figure 46.

(c) Stringer Flange: The maximum RMS strain for each NASTRAN analysis occurred at the mid point of the stringer tear strap, i.e., at the interface of the panel skin and the stringer flange. Figure 47 provides guidance on selection of stringer flange thickness. The thickness indicated in that figure is the sum of the skin and flange thickness.

The required thickness for sonic fatigue resistant design of fuselage skin-stringer structure are determined for a specific panel size and stringer web height - a, b, and h. Given a and b, the panel skin thickness is estimated from Figure 45. Figure 46 provides the ratio of stringer web thickness to the skin thickness for the given b/h. The stringer flange thickness is determined by subtracting the skin thickness from the total tear strap thickness determined from Figure 47 for the a x b panel.

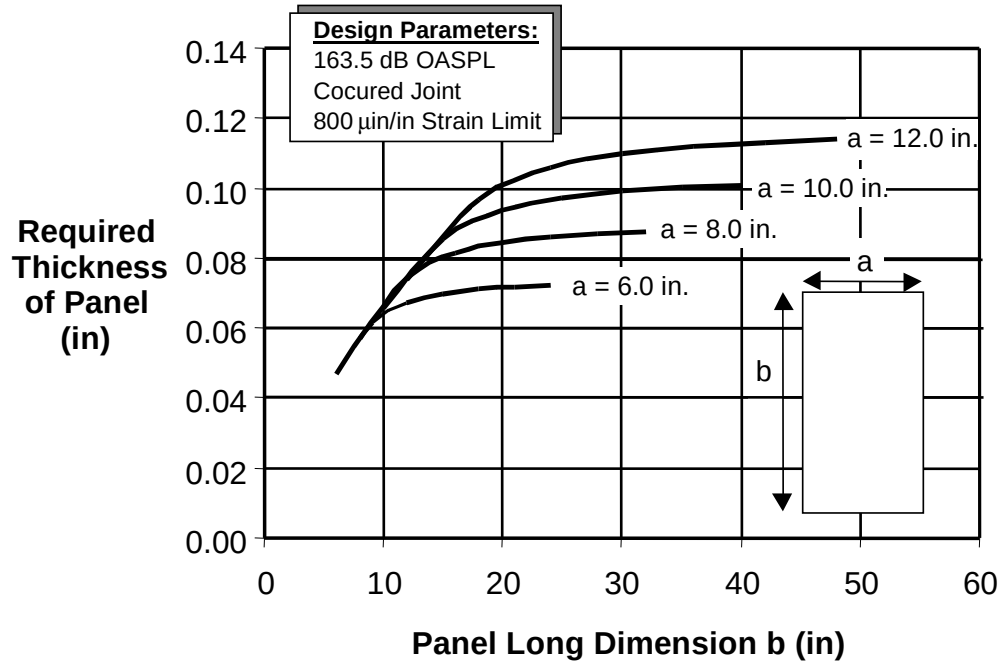

Figure 45 Required Panel Thickness for Sonic Fatigue Criteria (Skin/Stringer)

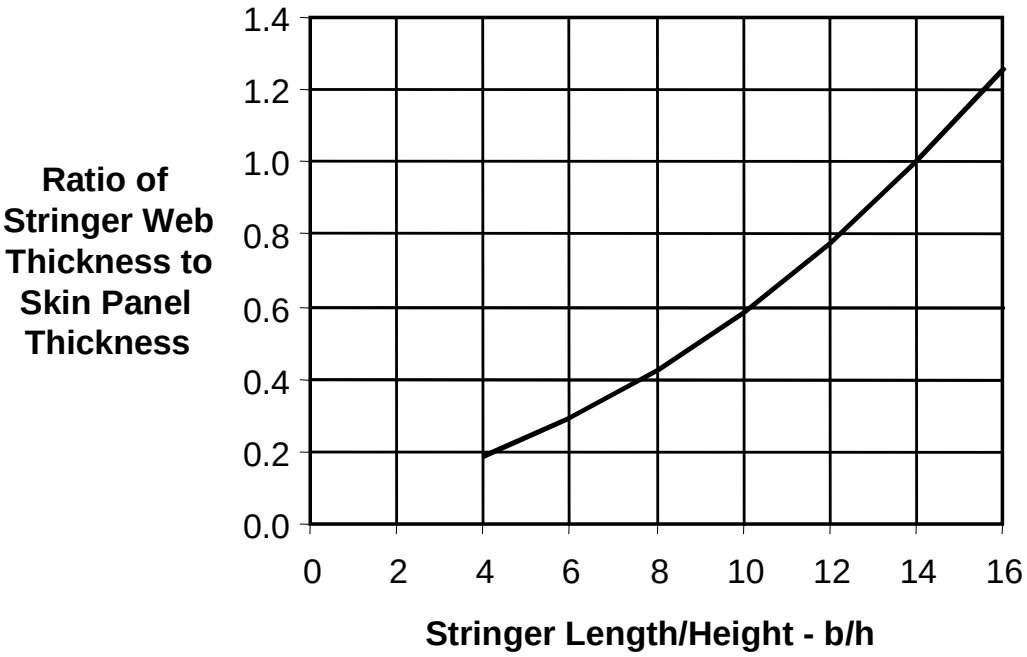

Figure 46. Stringer Requirements for Sonic Fatigue

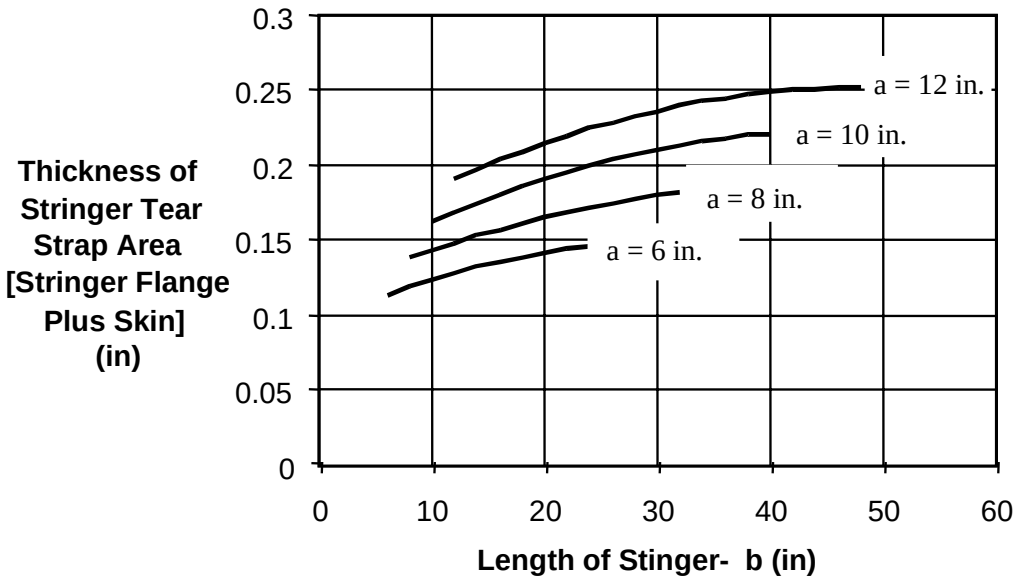

Figure 47 Stringer Flange Minimum Thickness

Verification

Four additional cases, not used in development of the guidelines, were analyzed by the defined process to assess the accuracy of the technique. Linear NASTRAN acoustic response analyses were performed and maximum RMS strain determined for the computed strain PSDs. Table 6 summarizes the input parameters, including thickness values determined by the sonic fatigue process, and the computed strains. Dimensions are in inches and strains in μin/in. The limit RMS strain is 800 μin/in.

Table 6 Sonic Fatigue Check Cases - Skin/Stringer

Parameter	Case 1	Case 2	Case 3	Case 4
Distance between stringers - a (in)	8.6	7	10	11
Length of stringers - b (in)	20	7	10	20
Height of stringer web - h (in)	1.724	1	1.5	1.724
Skin thickness (in)	0.088	0.052	0.0656	0.1
Stringer web thickness (in)	0.065	0.018	0.022	0.075
Stringer flange thickness (in)	0.0855	0.072	0.0976	0.1
Max RMS Strain - skin (μin/in)	441	**671**	**683**	530
Max RMS Strain - str. web (μin/in)	579	353	285	603
Max RMS Strain - str. flange (μin/in)	**684**	497	493	**781**

Computed RMS strain values were about 35 percent (Case 3, stringer web strain) to 97.5 percent (Case 4, stringer flange strain) of that limit value. Maximum strains for each case were 684 εin/in (Case 1 flange), 671 εin/in (Case 2 skin), 683 εin/in (Case 3 skin) and 781 εin/in (Case 4 flange). Therefore, the peak RMS strains were 2.5 to 16% below the limit strain. Case 1 is most representative of HSCT fuselage conceptual design. For that case, the design guidelines result in strain values 15 to 45% below the limit. For a specific design, further analysis may allow the removal of some weight, but such an effort is not warranted at this point in the development process.

PMC-TI Honeycomb Development

The second structural option for HSCT fuselage structure is a PMC-TI honeycomb panel configuration stiffened only by longitudinal frames. Sonic fatigue design curves were also developed for this configuration.

Panel Geometry

The slightly curved skin structure was again approximated as a flat panel and frames since the fuselage side between windows and floor, where acoustic levels are highest, is practically flat. The NASTRAN model (Figure 48) consists of 2660 nodes and 3515 finite elements (925 CHEXA solid elements representing the honeycomb core, 1702 quadrilateral plate elements modeling the face sheets and 888 plate elements for the frames). Design curves are intended to provide the minimum required thickness of the core (t_{core}) for a given distance between frames (b) and realistic face sheet thickness ($t_{facesheet}$).

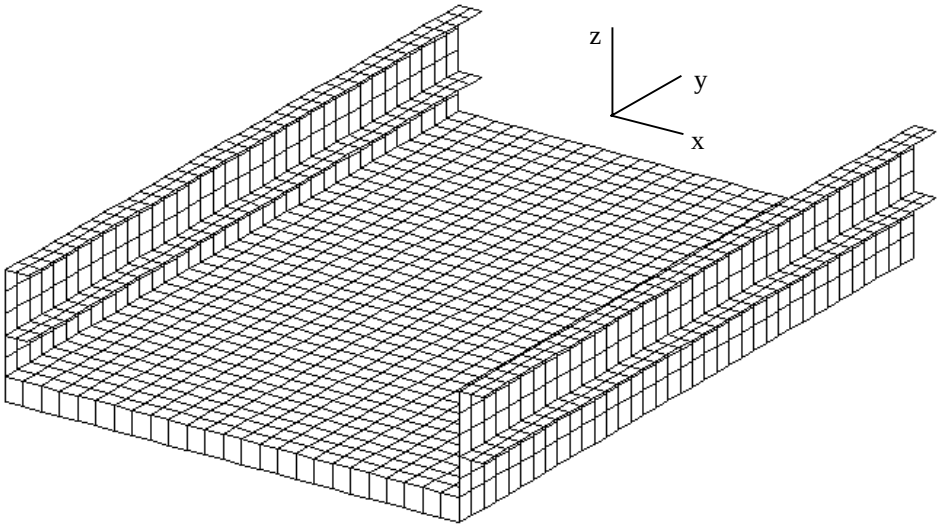

Figure 48 HSCT Fuselage PMC-TI Honeycomb Model

Analysis Procedure

Based on test data for the representative honeycomb beam specimen discussed in Section 3.0, a limit strain of 800 μin/in, the same value indicated for skin/stringer structure, is selected for HSCT honeycomb panel design. The basic analytic prediction criteria included in the skin/stringer studies were also employed for those of the honeycomb. Lightly damped (c/c_{cr} = 0.01) flat panels were subjected to the broadband noise described in section 2.0. Parametric NASTRAN linear acoustic response analyses were conducted on the model of Figure 48 to provide results used to develop the design curves. Symmetric and anti-symmetric boundary conditions were utilized at the ends of the model to represent a long expanse of the honeycomb structure. Highest stress and strain were computed for the anti-symmetric cases. Independent variables were the distance between frames (b) and the thickness of the face sheets ($t_{facesheet}$).

The model was consistent in size with the skin/stringer/frame model utilized for those studies. The ratio of panel length to distance between frames was 1.5. F-cross-section aluminum frames of 0.125 inch thickness were 5.172 inch high. Frame spacing of 10 to 40 inches were analyzed. The minimum IM7/PETI-5 face sheet thickness of 0.0416, representing eight 0.0052 inch plies, was analyzed as were 0.0624 inch twelve ply and 0.0832 inch sixteen ply configurations. Core thickness was varied to determine the minimum thickness required to limit both core and face sheet strains to the design value of 800 μin/in. Design curves were developed from these analytic results.

Results

Acoustic response analyses indicate that, as expected from the honeycomb beam testing, peak shear stress and strain in the core occurs near the interface with the substructure frame. Maximum face sheet stresses were shear values at the edge of the panel near the frames while highest normal stress, though less than the shear values, were at the center of the panel. Typically shear stress and strain of the core exceeded that of the face sheet. The exception was for cases with large frame spacing (40 inch) and thick core (>0.5 inch) where the face sheet strain was the designing parameter. Based on parametric linear NASTRAN analyses, the design curves of Figure 49 were developed to limit RMS strain in the honeycomb core and face sheets to 800 μin/in. The design guidelines can be used to determine the honeycomb geometry for a given frame spacing or to determine the maximum spacing for a specified honeycomb structure.

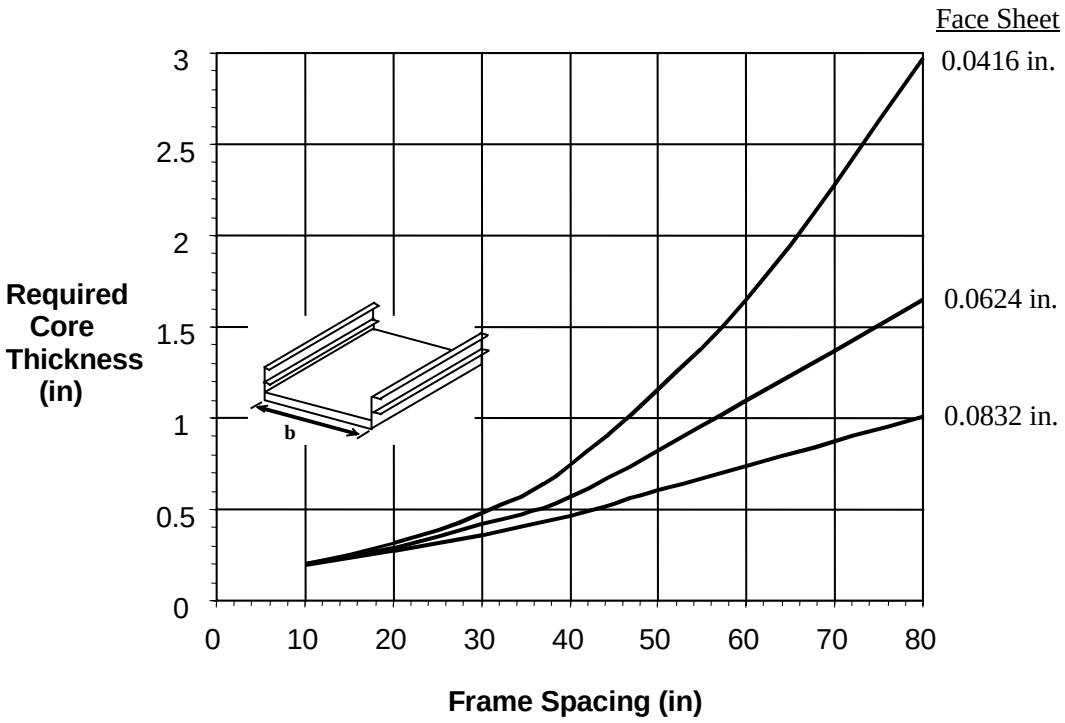

Figure 49 Required Honeycomb Core Thickness for Sonic Fatigue Criteria

Verification

Three cases, not used in development of the guidelines, were analyzed by the defined process to assess the accuracy of the technique (Table 7). Linear NASTRAN acoustic response analyses were performed and maximum RMS strain determined for the computed strain PSDs.

Case 1: The current HSCT fuselage Section 46 honeycomb panel design consists of a 0.55 inch core and 0.083 inch face sheets. From Figure 49, maximum strain should be considerably less than 800 μin/in for spacing up to 40 inches, the maximum analyzed in development of the curves. Extrapolation of the design curve indicates a maximum spacing of 50 inches and this configuration was analyzed. Results in Table 7 show that the maximum computed RMS strain is 751 μin/in or about 94% of the limit criterion.

Case 2: Based on Figure 49, a 36 inch honeycomb panel with 0.0416 inch face sheets should have a minimum core thickness of 0.63 inches to limit peak RMS strain to 800 μin/in. The results of linear NASTRAN analysis of this case verify this since the computed maximum RMS strain is 801 μin/in.

Case 3: Both previous cases analyzed configurations with relatively large distance between frames and with thick cores. Consequently, the face sheet strain exceeded that in the core. This case is selected to provide verification for small, thin panels in which core strain will be higher. For 12 inch spacing between frames, a core thickness

of 0.22 inch is sufficient regardless of the face sheet thickness. This is verified as shown in Table 7.

Table 7 Sonic Fatigue Check Cases - Honeycomb Panels

Parameter	Case 1	Case 2	Case 3
Distance between frames - b (in)	50	36	12
Thickness of face sheets (in)	0.083	0.0416	.0416
Thickness of honeycomb core (in)	0.55	0.58	0.22
Core Shear Strain - ε_{yz} (μin/in)	570	699	533
ε_{zx} (μin/in)	553	375	**735**
Face Sheet Strain - ε_x (μin/in)	478	403	246
ε_x (μin/in)	238	215	116
ε_{xy} (μin/in)	**751**	**801**	396

The case 1 panel is most representative of HSCT fuselage conceptual design, although the frame spacing (b) may not be representative since it was selected to provide limit strain based on the design curve (Figure 49).

Implications for HSCT Fuselage Design/Weight Penalties

These design requirements define minimum structural gage and, therefore, minimum weight required for an airframe that will withstand sonic loads throughout its service life. In high acoustic areas the minimum gage criteria shown in Tables 8 and 9 are required. The delta weight density values in those tables represent the increase in weight resulting from the minimum gage criteria, based on sonic fatigue considerations, compared to the baseline used by the HSR Fuselage ITD team prior to development of the sonic fatigue design guidelines.

Table 8 Minimum Gage Criteria for Skin/Stringer Fuselage Concept

Stringer Spacing (in)	Skin Thickness (in)	Flange Thickness (in)	Δ Weight per square foot (lb/sq ft)
8.6	0.09	0.08	0.21
12.0	0.10	0.13	0.33

Table 9 Minimum Gage Criteria for PMC Honeycomb Fuselage Concept

Core Thickness (in)	Frame Spacing (in)	Face Sheet Thickness (in)	Δ Weight per square foot (lb/sq ft)
0.55	40	0.069	0.22
0.55	50	0.083	0.34

Note: Frame spacing greater than 50 inches is not recommended in high acoustic areas

These criteria, based on sonic fatigue, were applied to the fuselage pathfinder designs presented during the 1998 HSR Fuselage team mid-year review. It was assumed that high acoustic impingement existed on the side of fuselage Section 43 due to a wake from the canard and on the sides and bottom of fuselage Section 46 as a result of engine exhaust noise. The changes shown in Table 10 are needed in the area below the window belt and the passenger floor for the skin/stringer design.

Table 10 Design Curves Needed for Fuselage Skin/Stringer Design

Section	Detail	Current Design Thickness (in)	Required Thickness (in)	Δ Weight per square foot (lb/sq ft)
43	Flange	0.04	0.05	0.014
46	Stringer Web	0.05	0.115	0.085

As noted from Figure 49, the honeycomb design curves, required core and facesheet thickness increase rapidly for frame spacing in excess of 40 inches. The current design for fuselage Section 46 is adequate for sonic fatigue resistance. In order to accommodate a frame spacing of 80 inches in Section 43, the side fuselage areas would require increases shown in Table 11.

Table 11 Design Changes Needed for Section 43 PMC Honeycomb Design

Detail	Current Design Thickness (in)	Required Thickness (in)	Δ Weight per square foot (lb/sq ft)
Facesheets	0.055	0.0832	0.47
Core	0.25	1.0	1.51
			Total = 1.98

HSCT Wing Design Requirements

Preliminary sonic fatigue analysis was performed on the HSCT wing design. This analysis was based on the HSCT design sonic loading due to inlet noise, interim design curves developed for PMC-TI honeycomb structure (applied previously to fuselage panels) and NASTRAN/PATRAN parametric linear response procedures. The objective was to provide guidance to the HSR Wing Design Team and to provide comments on the current design.

Sonic Loading

Prior to reduction of TU-144 flight data, the inlet sonic loading was based on supersonic tactical aircraft measurements. The maximum predicted level was 153.5 dB OASPL, including a 3.5 dB factor of safety, with the octave band spectrum shape shown in Figure 4. During TU-144 flight tests, considerably higher levels were measured near the lower surface of the wing. Figure 50 shows that realistic levels as high as 160.7 dB were measured. Considering the factor of safety, the fuselage design level of 163.5 dB and the associated spectrum shape are more appropriate than the predicted 153.5 dB and the higher values are, therefore, utilized for preliminary wing analyses.

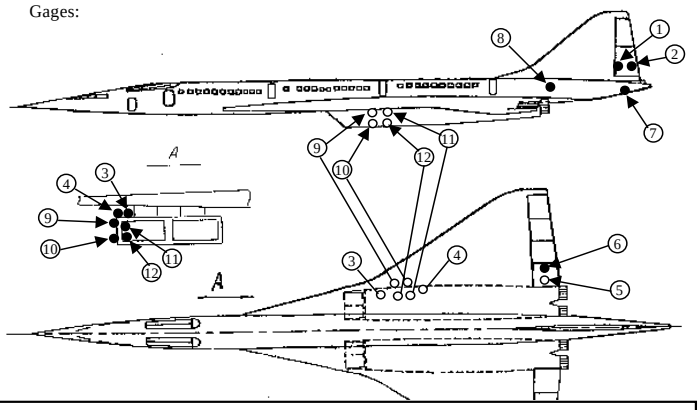

Gage	Location	Max OASPL (dB)
3	Inlet Exterior	160.3*
4	Inlet Exterior	156.5**
5	Flap (Lower)	154.0
6	Flap (Upper)	145.7
9	Inlet Exterior	152.4
10	Inlet Exterior	160.7

* One 166.4 dB Measurement Not Typical

** One 163.4 dB Measurement Not Typical

Figure 50 Sonic Loading on TU-144 Wing

Analysis/Results

The design curves developed for HSCT fuselage honeycomb panels (Figure 49), based on the 163.5 dB design SPL spectrum, were used for preliminary wing analyses. A typical wing frame spacing of 40 inches was assumed. Five areas of the lower wing surface were selected as potentially susceptible to sonic fatigue due to local geometry and noise impingement. Those areas are designated A through E in Figure 51. These preliminary analyses do not consider sonic contours but assume that the maximum noise level is applicable to all locations on the lower wing surface. Area E, composed of three adjacent wing boxes, is subjected to the highest loading and is most susceptible. In particular, WSL_12 is most susceptible since it has both the smallest face sheet thickness and core thickness in that area of the wing.

Area	Wing Station	Face Sheet t (in)	Core t (in)
A	WSL_34	0.307	0.234
B	WSL_1	0.042	1.006
C	WSL_48	0.073	0.372
D	WSL_49	0.094	0.258
E	WSL_10	0.166	1.008
	WSL_11	0.114	1.004
	WSL_12	0.114	1.000

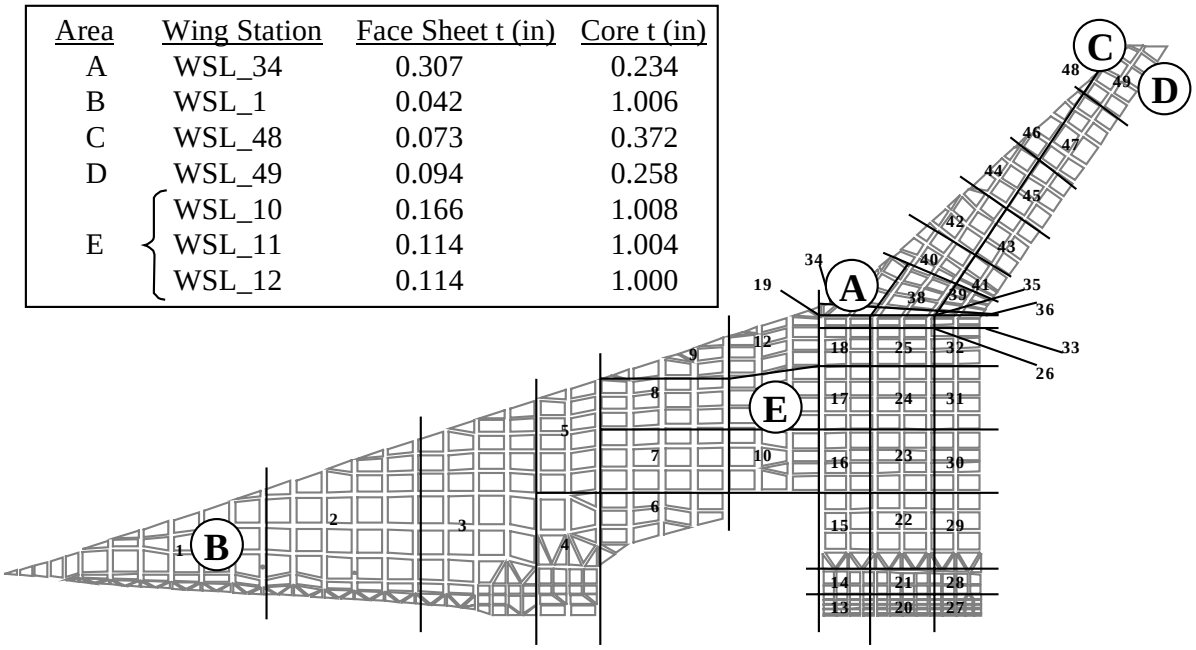

Figure 51 HSCT Lower Wing Surface Design Zones

Required core thickness of the various areas for sonic fatigue resistant design of the honeycomb wing panels were determined from the design curves (Figure 49) and validated by NASTRAN linear response analyses. From the required thickness values shown in Table 12 and NASTRAN analysis results in Table 13, the current wing design at locations A and C are questionable, and that at location D is marginal.

Table 12 Wing Sonic Fatigue Requirements

Case No.	Location on Wing	Face Sheet Thickness (in)	Design Core Thickness (in)	Required Core Thickness (in)
A	WSL_34	0.307	0.234	Outside Range
B	WSL_1	0.042	1.006	0.68
C	WSL_48	0.073	0.372	0.50
D	WSL_49	0.094	0.258	~ 0.25 - 0.27
E	WSL_12	0.114	1.000	0.20

Table 13 Wing NASTRAN Analysis Results

Case No.	Maximum Strain (μin/in) Core	Face Sheet	Comment
A	1165	266	Thicker Core Required
B	372	589	Acceptable Design
C	856	788	Exceeds Allowable; Increase Core
D	820	630	Marginal Design
E	335	225	Acceptable Design

NASTRAN analyses of Cases A and C were re-run with 0.5 inch core thickness to verify the acceptability of that re-design. Maximum computed RMS strains were 640 μin/in in the core for both cases. Face sheet strains were 143 μin/in for Case A and 703 μin/in for Case C. Therefore, peak RMS strains were within the 800 μin/in endurance limit, validating the proposed re-design.

Structural Conclusions / Recommendations

The following conclusions are based on the sonic fatigue analyses:

1. The skin/stringer fuselage design requires little modification. Some design detail to stabilize the edge of the stringer flanges would reduce the penalty in strain allowable for the high Kt at the edge of the stringer flange.
2. Frame spacing in excess of 40-50 inches for the fuselage PMC honeycomb concept is not recommended due to high vibratory response associated with the large unsupported panels.
3. Core thickness less than 0.5 inches should be avoided in the wing honeycomb design.

6.0 PASSIVE SONIC FATIGUE REDUCTION TECHNIQUES

The objective of these analytic and experimental studies was to develop passive techniques / structural treatments to improve sonic fatigue resistance for critical structural components of the High Speed Civil Transport.

Damping Analysis

An analysis was performed to determine the extent of damping which can be obtained from the addition of damping layers in the fuselage skin laminate or the addition of damped, segmented stiffeners. Four different methods of damping the structure were investigated. These included: (1) adding constrained layer damping to the inside skin surface, (2) adding damped longitudinal stiffness in the center of the skin panels, (3) adding transverse damped stiffness to the skin panels, and (4) the configuration shown in Figure 52. A summary of strain energies and weight penalties for the four concepts investigated is shown in Table 14. The best results were obtained for the Figure 52 configuration, which added damped stiffeners on the skin panels and augmented original stringers. The damped stringers were mounted on the skin panels perpendicular to the original stringers. The augmentation of the original stringers, also shown in the Figure 52 inset, consisted of attaching an inverted damped T shaped stiffener to the original stringers. With a damping material shear modulus of 500 psi, the percent element strain energy found in the damping layer (which is a measure of available damping) was 7.04% and 7.14% for a global and local panel mode respectively.

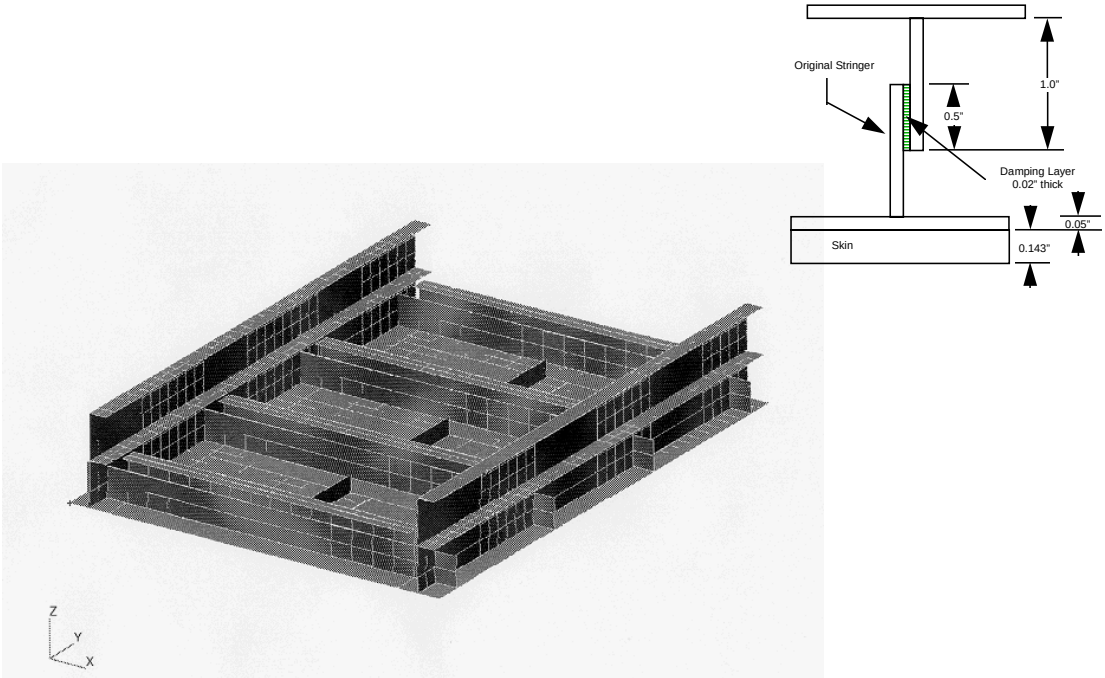

Figure 52 Damped Cross Stiffeners with Augmented Stringers

Table 14 Summary of Damping Concepts

Concept	% Element Strain Energy Global Mode	% Element Strain Energy Local Mode	Weight Penalty (lbs/ft^2)
Constrained Damping Layer	3.08	2.69	1.50
Longitudinal Damping Stiffeners	0.69	0.72	0.88
Cross-Panel Damping Stiffeners	5.82	4.21	0.32
Cross-Panel Damping Stiffeners / Augmented Stringers	7.03	7.14	1.18

A flat panel finite element model developed by Boeing-St. Louis was used for these studies. Some of the more promising passive reduction concepts were checked out on the curved fuselage skin model prepared by Lockheed-Martin. More details on the analysis performed may be found in Reference [g]. The result of this preliminary analysis was to verify the potential reduction in sonic fatigue response, and hence weight, which could be achieved by addition of damping treatment.

AEDC Testing

The objective of this effort was to develop lightweight passive damping concepts to reduce sonic fatigue risk and to test sample sub-components. The target weight of the treatment is 0.5 lb/sq ft or less. The two most promising concepts, identified by Boeing, St. Louis, are shown in Figure 53. The first is a constrained layer damping treatment and the second is an integral damped layer treatment. Analysis of the constrained layer damping concept indicated damping values of about 2-3% could be achieved, while values of about 4-5% could be achieved for the integral damped layer concept. Skin/stringer panels were tested in the AEDC Wind Tunnel in May/June 1998 (Test 1) and September 1998 (Test 2). The bare and treated honeycomb panel was also tested during Test 2. A treatment similar to the constrained layer concept shown above was added to a honeycomb panel that was tested in the interior noise boundary layer measurements testing performed at AEDC. Only the constrained layer concept was verified by a test, since the integral layer concept would require splitting the one inch thick titanium core and adding additional damping material constraining / face sheets. A modal tap test was performed on the panel before and after treatment to determine its effect. The results are shown in Figure 54 along with a sketch showing a cross section of the tested treatment. Figures 55 and 56 show the effect of the damping treatment on measured sound intensity at Mach 0.8 and 1.2. An effective damping treatment for PMC honeycomb panels was developed and its effectiveness verified by test.

For comparison, Mach 1.2 data for the tested skin/stringer panel is shown in Figure 57 and a summary of the damping results from 500 to 5000 Hz for both skin/stringer and honeycomb panels is shown in Table 15. The damping was more effective on the

skin/stringer panel than on the honeycomb panel with three times more intensity reduction per unit weight increase. However, the honeycomb test panel had a relatively thick core (1 inch) and anticipated reduction in response due to damping is much less than it would be for thinner core structure. The lack of performance of damping on the honeycomb panel is also attributed to its small size and high stiffness. A more effective damping treatment could be designed for larger panels. The weight of the treatment on the honeycomb panel (0.6 lb/sq ft) was slightly heavier than the target, since loaded foam core was used because of its availability. These test results are very limited and considerably more testing would be required to characterize damping effectiveness.

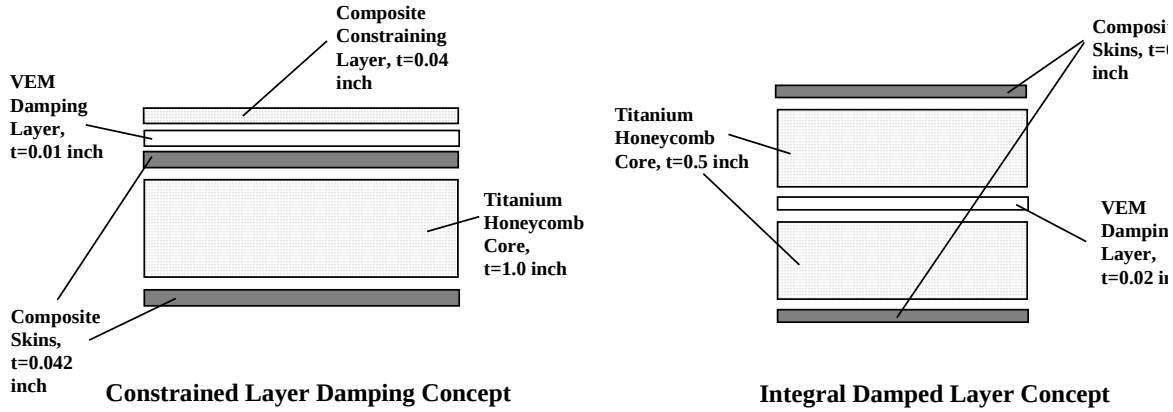

Figure 53 Damping Concepts

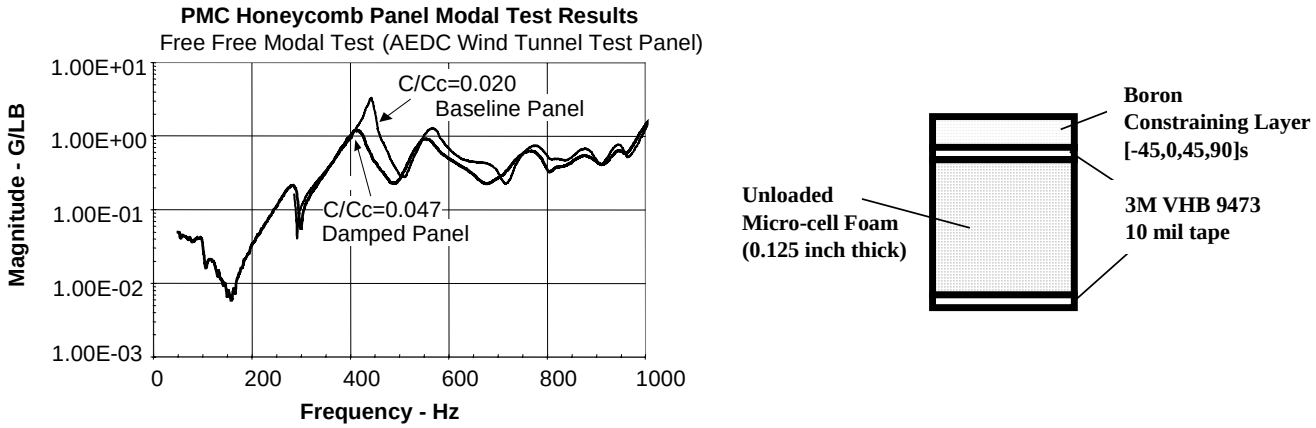

Figure 54 Results of Modal Tap Test of Honeycomb Panel

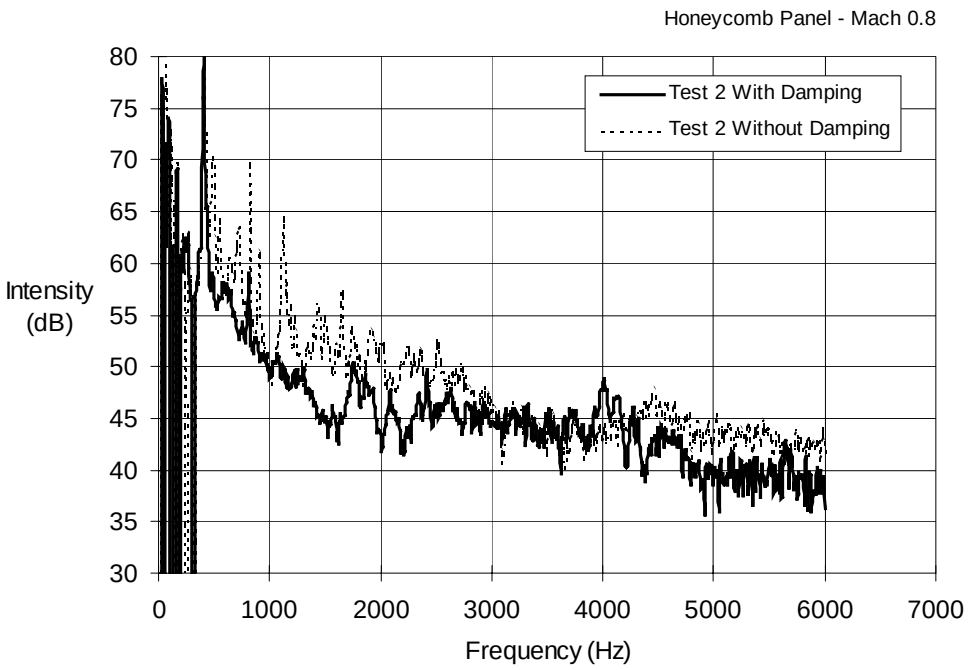

Figure 55 Effect of Damping on Honeycomb Test Panel - Mach 0.8

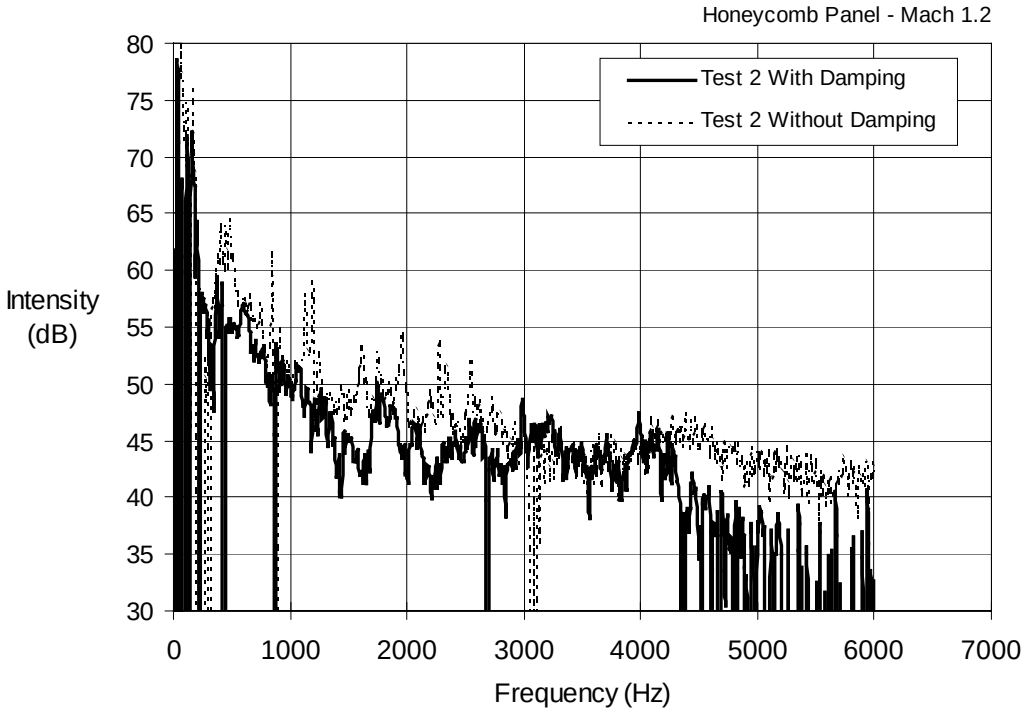

Figure 56 Effect of Damping on Honeycomb Test Panel - Mach 1.2

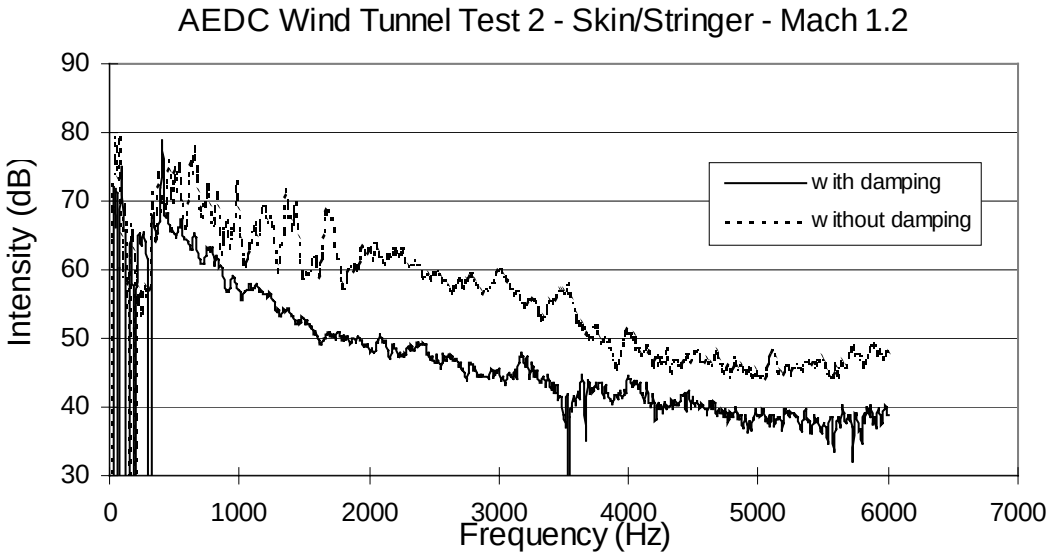

Figure 57 Effect of Damping on Skin/Stringer Test Panel - Mach 1.2

Table 15 Damping Results from AEDC Testing

Configuration	Average Delta Intensity Level (dB)	Delta Surface Weight - Treatment weight / Panel area (lb/sq in.)	Delta Intensity Level / Delta Surface Weight (dB/lb)
Honeycomb	4.3	0.5675	7.58
Skin/Stringer	9.475	0.4351	21.78

7.0 RECOMMENDATIONS

The HSR Sonic Fatigue program provided considerable useful information, which if extended, would be even more valuable. Despite cessation of this program, the following tasks are recommended for continuing effort.

1. Further reduction of the TU-144 flight data is required to determine the distribution of sonic loads on all high acoustic zones of the airframe, i.e., to develop a sonic load map of the airframe. These data can then be scaled based on HSCT expected engine flow rates, areas and temperatures to yield more accurate sonic load predictions.

2. Further characterization of strain - cycles to failure (ε-n) data for IM7/PETI-5 material requires additional testing at elevated temperatures and with static pre-loads applied. Testing should be conducted at 500^{o}F because the reduction in properties at 350^{o}F (Figure 1 and 28) is within the scatter band of the room temperature data. These tests would enhance the possibility of this material being used on other programs.

3. Development of the NASTRAN DMAP solution for non-linear dynamic response and the life calculation nCode fatigue module should be completed as a basis for the performance of more accurate sonic fatigue analyses. Current linear analysis and the resulting uncertainties in results lead to conservative, relatively heavy designs. These improved methods are needed for programs other than HSR and would be of immediate value.

4. Sonic fatigue analyses should continue in support of the structural design efforts that continue to evaluate critical fatigue details in the design concepts. These include the close-outs at the edges of PMC-TI honeycomb panels which are prone to adhesive shear failures in areas of high dynamic response of large panels.

8.0 REFERENCES

a) Boeing Report CRAD-9408-TR-3863, “HSR Airframe Technology, Airframe Materials & Structures, 4.2.7 Structural Acoustics, 1997 Sonic Fatigue Final Report,” The Boeing Company, 14 November 1997.

b) McDonnell Douglas Aerospace Report No. CRAD-9408-TR-2058, “Prediction of Engine Inlet Acoustic Loads, High Speed Research-Airframe Technology,” Contract ZA0227, 10 October 1996.

c) Green, M.W., “AV-8B Sonic and Vibration Fatigue Loads Report,” MDC A6392, Rev. C, 31 July 1995.

d) Shunaev, V.P., Feigenbaum, U.M., Minaev, R.N., Luchinsky, M.N., Rackl, R.G., Rizzi, S.A., “Results of acoustic loads measurements on the Tu-144LL airplane structure - Experiment 2.1,” ANTK Tupolev, Moscow, Russia, 23 March 1998.

e) Jacobson, M.J., “Advanced Composite Joints; Design and Acoustic Fatigue Characteristics,” AFFDL-TR-71-126, Apr 1972.

f) Holehouse, I., “Sonic Fatigue Design Techniques for Advanced Composite Aircraft Structures,” AFWAL-TR-80-3019, April 1980.

g) McDonnell Douglas Aerospace Report No. CRAD-9408-TR-2881, “HSCT Passive Control - Structure Design - Part I, High Speed Research - Airframe Technology,” Contract ZA0227, 20 January 1997.

REPORT DOCUMENTATION PAGE

Form Approved
OMB No. 0704-0188

1. REPORT DATE *(DD-MM-YYYY)*	2. REPORT TYPE	3. DATES COVERED *(From - To)*
01- 04 - 2005	Contractor Report	

4. TITLE AND SUBTITLE
High Speed Research Program Sonic Fatigue Summary Report

5a. CONTRACT NUMBER
NAS1-20220

5b. GRANT NUMBER

5c. PROGRAM ELEMENT NUMBER

6. AUTHOR(S)
Beier, Theodor H.; and Heaton, Paul

5d. PROJECT NUMBER

5e. TASK NUMBER

5f. WORK UNIT NUMBER
537-06-37-20

7. PERFORMING ORGANIZATION NAME(S) AND ADDRESS(ES)
NASA Langley Research Center
Hampton, VA 23681-2199
The Boeing Company
St. Louis, MO

8. PERFORMING ORGANIZATION REPORT NUMBER

9. SPONSORING/MONITORING AGENCY NAME(S) AND ADDRESS(ES)
National Aeronautics and Space Administration
Washington, DC 20546-0001

10. SPONSOR/MONITOR'S ACRONYM(S)
NASA

11. SPONSOR/MONITOR'S REPORT NUMBER(S)
NASA/CR-2005-213742

12. DISTRIBUTION/AVAILABILITY STATEMENT
Unclassified - Unlimited
Subject Category 71
Availability: NASA CASI (301) 621-0390

13. SUPPLEMENTARY NOTES
Langley Technical Monitor: Stephen A. Rizzi
An electronic version can be found at http://ntrs.nasa.gov

14. ABSTRACT

The objective of this sonic fatigue summary is to provide major findings and technical results of studies, initiated in 1994, to assess sonic fatigue behavior of structure that is being considered for the High Speed Civil Transport (HSCT). High Speed Research (HSR) program objectives in the area of sonic fatigue were to predict inlet, exhaust and boundary layer acoustic loads; measure high cycle fatigue data for materials developed during the HSR program; develop advanced sonic fatigue calculation methods to reduce required conservatism in airframe designs; develop damping techniques for sonic fatigue reduction where weight effective; develop wing and fuselage sonic fatigue design requirements; and perform sonic fatigue analyses on HSCT structural concepts to provide guidance to design teams. All goals were partially achieved, but none were completed due to the premature conclusion of the HSR program. A summary of major program findings and recommendations for continued effort are included in the report.

15. SUBJECT TERMS
High Speed Research Program; Structural Acoustics; Sonic Fatigue

16. SECURITY CLASSIFICATION OF:			17. LIMITATION OF ABSTRACT	18. NUMBER OF PAGES	19a. NAME OF RESPONSIBLE PERSON
a. REPORT	b. ABSTRACT	c. THIS PAGE			STI Help Desk (email: help@sti.nasa.gov)
					19b. TELEPHONE NUMBER *(Include area code)*
U	U	U	UU	66	(301) 621-0390